

# JGR Biogeosciences

## RESEARCH ARTICLE

10.1029/2021JG006411

### Key Points:

- Temperature is a stronger driver of CO<sub>2</sub> fluxes in disturbed peatlands compared with intact ones
- Remotely sensed land surface temperature (LST) is a strong predictor of in situ thermal conditions in disturbed peatlands
- Remotely sensed LST has a great potential for modeling ecosystem respiration in disturbed peatlands

### Supporting Information:

Supporting Information may be found in the online version of this article.

### Correspondence to:

I. Burdun,  
[iuliia.burdun@ut.ee](mailto:iuliia.burdun@ut.ee)

### Citation:

Burdun, I., Kull, A., Maddison, M., Veber, G., Karasov, O., Sagris, V., & Mander, Ü. (2021). Remotely sensed land surface temperature can be used to estimate ecosystem respiration in intact and disturbed northern peatlands.

*Journal of Geophysical Research: Biogeosciences*, 126, e2021JG006411.  
<https://doi.org/10.1029/2021JG006411>

Received 21 APR 2021

Accepted 14 OCT 2021

### Author Contributions:

**Conceptualization:** Iuliia Burdun, Ain Kull, Martin Maddison, Valentina Sagris, Ülo Mander

**Data curation:** Iuliia Burdun, Ain Kull, Martin Maddison, Gert Veber

**Formal analysis:** Iuliia Burdun, Martin Maddison

**Funding acquisition:** Ülo Mander

**Investigation:** Iuliia Burdun, Ain Kull, Martin Maddison, Gert Veber, Oleksandr Karasov, Valentina Sagris, Ülo Mander

**Methodology:** Iuliia Burdun, Ain Kull, Martin Maddison, Gert Veber, Oleksandr Karasov, Ülo Mander

**Project Administration:** Ain Kull, Ülo Mander

**Resources:** Ain Kull, Valentina Sagris, Ülo Mander

**Software:** Iuliia Burdun

## Remotely Sensed Land Surface Temperature Can Be Used to Estimate Ecosystem Respiration in Intact and Disturbed Northern Peatlands

Iuliia Burdun<sup>1</sup> , Ain Kull<sup>1</sup> , Martin Maddison<sup>1</sup> , Gert Veber<sup>1</sup>,  
Oleksandr Karasov<sup>1</sup> , Valentina Sagris<sup>1</sup> , and Ülo Mander<sup>1</sup> 

<sup>1</sup>Department of Geography, Institute of Ecology & Earth Sciences, University of Tartu, Tartu, Estonia

**Abstract** Remotely sensed land surface temperature (LST) enables global modeling and monitoring of CO<sub>2</sub> fluxes from peatlands. We aimed to provide the first overview of the potential for using LST to monitor ecosystem respiration ( $R_{\text{eco}}$ ) in disturbed (drained and extracted) peatlands. We used chamber-measured data (2017–2020) from five disturbed and two intact northern peatlands and LST data from Landsat 7, 8, and MODIS missions. First, we studied the strength of the relationships between fluxes and their in situ drivers (i.e., thermal and moisture conditions). Second, we examined the association between LST and in situ temperatures. Third, we compared chamber-measured  $R_{\text{eco}}$  with the modeled  $R_{\text{eco}}$  driven by in situ measured water table depth and (a) in situ measured surface temperature and (b) remotely sensed MODIS LST data. In situ temperatures were a stronger driver of CO<sub>2</sub> fluxes in disturbed sites (repeated measures correlation  $\text{rmR} = 0.8\text{--}0.9$ ) than in intact ones ( $\text{rmR} = 0.5\text{--}0.8$ ). LST had a higher association with in situ measured temperatures in disturbed sites (mean  $\text{rmR} = 0.79$  for MODIS) and weaker in the intact (hummocks and hollows) peatlands (mean  $\text{rmR} = 0.38$  for Landsat and 0.48 for MODIS).  $R_{\text{eco}}$  models driven by MODIS LST and in situ surface temperature yielded similar accuracy:  $R^2$  was 0.27, 0.66, and 0.67 and 0.29, 0.70, and 0.66 for intact and for drained and extracted sites, respectively. Overall, these findings suggest the applicability of LST as a proxy of the thermal regime in  $R_{\text{eco}}$  models, particularly for disturbed peatlands.

**Plain Language Summary** Organic carbon (C) in the peat layer of peatlands has been accumulating for thousands of years. Under anthropogenic impacts, such as drainage for forestry, agriculture, or peat extraction, peatlands start releasing the accumulated C back into the atmosphere as CO<sub>2</sub> and CH<sub>4</sub> much faster than historical rates of C accumulation. CO<sub>2</sub> and CH<sub>4</sub> are the potent greenhouse gases that lead to climate warming. The thermal regime is among the main factors controlling CO<sub>2</sub> and CH<sub>4</sub> fluxes in peatlands. In this study, we demonstrated the potential of satellite thermal data for monitoring CO<sub>2</sub> fluxes from intact and disturbed peatlands. We used a long-term (2017–2020) data set of CO<sub>2</sub> data measured in seven Estonian peatlands. The thermal regime explains CO<sub>2</sub> fluxes. Also, satellite thermal data better represent both the thermal regime and CO<sub>2</sub> fluxes in disturbed rather than in intact peatlands. Furthermore, we modeled CO<sub>2</sub> fluxes from natural and disturbed peatlands: first, with thermal data measured in the field, and second, with satellite thermal data. Both models yielded similar prediction accuracy, which suggests that satellite thermal data have the potential to be used for modeling CO<sub>2</sub> fluxes from peatlands with a varying level of disturbance.

## 1. Introduction

Peatlands cover only ~3% of the global land area (J. Xu et al., 2018), but they store 21% of global terrestrial soil carbon (C) (Scharlemann et al., 2014), which is double the amount in the world's forests (Pan et al., 2011). Approximately 80% of peatland C stock is stored in peatlands north of 45°N (Yu et al., 2010). Historically, intact northern peatlands have acted as a vast C sink with an estimated average rate of C accumulation of 18.6 g/m<sup>2</sup> per year (Yu, 2011).

Intact peatlands bind atmospheric CO<sub>2</sub> as C within peat (Clymo et al., 1998; Salm et al., 2012). However, peatlands also lose C through CH<sub>4</sub> emissions due to shallow (ground-) water table depths (WTDs) and anoxic conditions in the peat layer (Waddington & Roulet, 2000). CH<sub>4</sub> has a more significant radiative efficiency than CO<sub>2</sub> but a much shorter lifetime in the atmosphere (Change, 2013). Therefore, over a millennial time

**Supervision:** Valentina Sagris, Ülo Mander

**Validation:** Iuliia Burdun, Ain Kull,

Gert Veber, Oleksandr Karasov

**Visualization:** Iuliia Burdun

**Writing – original draft:** Iuliia Burdun

**Writing – review & editing:** Iuliia Burdun, Ain Kull, Martin Maddison, Gert Veber, Oleksandr Karasov, Valentina Sagris, Ülo Mander

scale, intact peatlands have a cooling effect on the Earth's climate, despite being a source of CH<sub>4</sub> (Günther et al., 2020).

Over the past three centuries, human activity and a warming climate have lowered WTD in peatlands, leading to the oxidation of the peat layer (Kotta et al., 2018; Leifeld et al., 2019; Regan et al., 2019; Swindles et al., 2019). In drained peatlands, the groundwater level has fallen and such peatlands consequently have a thicker aerobic layer. In extracted peatlands, in addition to increased drainage, the vegetation layer has also been removed. Under warmer oxic conditions, the peat layer decomposes and releases accumulated C as CO<sub>2</sub> (Hanson et al., 2020; Rinne et al., 2020; Salm et al., 2009; Waddington et al., 2001). The rate of C loss can be 4.5–18 times faster than historical rates of C accumulation (Hanson et al., 2020). Currently, disturbed peatlands account for up to 10% of the global anthropogenic CO<sub>2</sub> emissions annually (Leifeld & Menichetti, 2018). Hence, disturbed peatlands are a significant source of CO<sub>2</sub> and have a long-term impact on climate warming (Leifeld et al., 2019; Ojanen et al., 2013). Notably, because of the CO<sub>2</sub> emissions from disturbed peatlands, the global peatland biome is expected to shift from sink to source in this century (Leifeld et al., 2019; Loisel et al., 2021).

CO<sub>2</sub> exchange, particularly ecosystem respiration ( $R_{eco}$ ), strongly depends on the climatic conditions of disturbed peatlands, including soil and air temperatures (Lloyd & Taylor, 1994; Maljanen et al., 2010; Veber et al., 2018). For example, a temperature-dependent function is widely used to model spatial and temporal  $R_{eco}$  from intact and disturbed peatlands (Alm et al., 2007; Bubier et al., 2003; Järveoja et al., 2020; Lafleur et al., 2001). In previous studies, C fluxes were shown to have positive exponential relationships with peat temperatures at different depths, including –20 cm (Helbig et al., 2019), –10 cm (Davidson et al., 2019), and –5 cm (Acosta et al., 2017), as well as with surface temperature (X. Huang et al., 2021). However, owing to a limited spatial coverage of in situ temperature measurements, the modeling of C fluxes is only possible at the plot scale. To overcome this limitation, remotely sensed parameters, including land surface temperature (LST), have been applied to allow a global modeling of  $R_{eco}$  in peatlands (Lees et al., 2018).

Rahman et al. (2005) were among the first researchers to apply remotely sensed data for  $R_{eco}$  modeling. They found that MODIS LST had an exponential relationship with  $R_{eco}$  over the wide range of North American land covers, and furthermore, this relationship varied between land covers. Later, Kimball et al. (2009) developed a terrestrial C flux model driven by remotely sensed inputs for boreal biomes; however, none of the validation sites were located in peatland. Subsequently, remotely sensed data were actively used to model C fluxes mainly for forest land covers (Crabbe et al., 2019; N. Huang et al., 2014, 2015; Jägermeyr et al., 2014; Olofsson et al., 2008; Tang et al., 2011; Wu et al., 2014; Xiao et al., 2010). The major part of these studies utilized MODIS data with a coarse spatial resolution (1 km for LST and 250 and 500 m for vegetation indices) with C data measured at eddy covariance towers and by chambers. So far, we know of only two studies that have utilized remotely sensed data of a higher spatial resolution, 30 m (Landsat), for CO<sub>2</sub> fluxes estimation. The first study was conducted over beech forest (Crabbe et al., 2019) and the second, over forested peatland (C. Xu et al., 2020).

The relationships between  $R_{eco}$  and remotely sensed LST in peatlands have received much less research attention than other ecosystems. Schubert et al. (2010) reported strong relationships between MODIS LST and  $R_{eco}$  in different types of peatlands, including bog (precipitation fed) and fen (additionally fed with groundwater and sometimes surface runoff). Later, Y. Gao et al. (2015) and Ai et al. (2018) developed models for  $R_{eco}$  simulation driven by MODIS LST and enhanced vegetation index (EVI). Those models were validated over large areas and diverse land covers, including marshes and wetlands, and both studies supported the existence of a strong relationship between  $R_{eco}$  and LST. More recently, Park et al. (2020) and Junttila et al. (2021) applied MODIS LST to estimate  $R_{eco}$  in tropical and northern peatlands, respectively. The case study on northern peatlands only included five peatlands (four fens and one bog), yet it demonstrated that the performance of LST varies between peatland types (Junttila et al., 2021).

Despite the progress made in estimating  $R_{eco}$  with remotely sensed data, much uncertainty remains regarding the strength of the relationships between  $R_{eco}$  and LST in disturbed (drained and extracted) peatlands. To our knowledge, no study has specifically addressed the applicability of LST for modeling CO<sub>2</sub> fluxes in such peatlands. We present the first attempt to fill this knowledge gap to tap into the potential of remotely sensed LST, which is especially urgent, given the need to manage substantial CO<sub>2</sub> emissions from disturbed

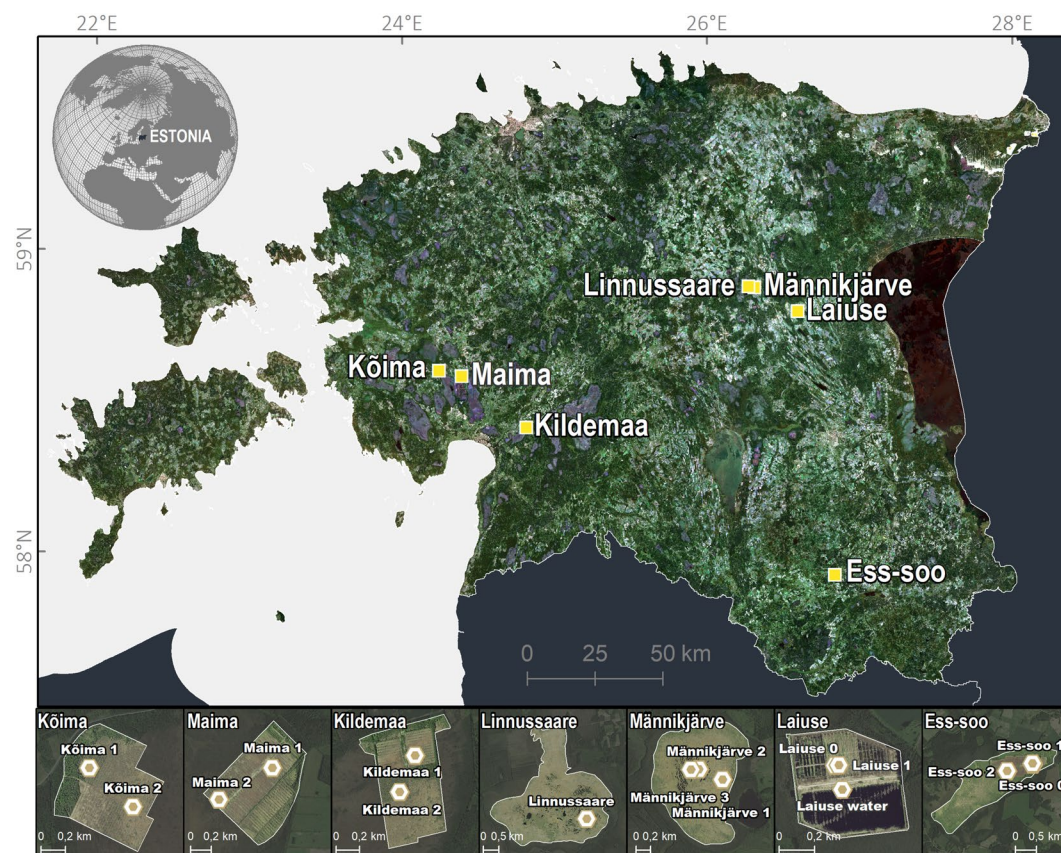


**Figure 1.** The study area includes seven boreal peatlands located in Estonia. The main panel shows a true-colored cloudless mosaic of Landsat 8 obtained in the summer of 2018. The lower small panels show the locations of sites where ecosystem respiration was measured. Orthophotos for the summers of 2019 and 2020 are presented in the lower small panels (Estonian Land Board, 2020).

peatlands. This article aims to quantitatively assess relationships between  $R_{eco}$  and remotely sensed LST in disturbed and intact northern peatlands. We evaluated the applicability of LST for  $R_{eco}$  modeling in comparison with in situ measured surface temperature. Overall, we used  $R_{eco}$  data from seven Estonian peatlands. Five of these peatlands experienced peat extraction activity and water drainage in the past, while the other two peatlands are natural bog sites. Flux data were measured using closed chambers during the snow-free period in March–November (2017–2020). We studied relationships between in situ measured temperatures and LST data from MODIS Terra, Landsat 7, and Landsat 8 satellites. Finally, we examined the applicability of MODIS LST for  $R_{eco}$  modeling and compared the performance of this model with the model using in situ measured surface temperature.

## 2. Materials and Methods

### 2.1. Study Area

We collected  $R_{eco}$  data in seven boreal peatlands (Figure 1) with various drainage conditions (Table 1) in Estonia. In addition to  $CO_2$  data, we measured  $CH_4$  fluxes (Burdun et al., 2021). The study area has a temperate climate with the long-term (1991–2020) mean annual temperature and precipitation of 7°C and 662 mm, respectively (Estonian Weather Service, 2021). Figure 1 shows the location of study peatlands (upper panel) and zoomed-in orthophotos for each peatland (bottom panels).

Ess-soo bog in southwest Estonia is of limnogenic origin. Its peat layer varies from 4 to 6 m, but in an abandoned (in 1994) milled peat extraction site, it varies from 2 to 4 m. Vegetation cover in the abandoned milled

**Table 1**  
Overview of Peatland Sites

Sampling site	Peatland condition	Number of chambers (ch.) and microtopographic units	Dominant species	Lat.	Long.
Ess-soo					
Ess-soo 0	Extracted	4 ch.	<i>Eriophorum vaginatum</i> , <i>Calluna vulgaris</i> , <i>Vaccinium uliginosum</i> , <i>Polytrichum strictum</i> , <i>Betula pubescens</i> , and <i>Pinus sylvestris</i>	57.914	26.697
Ess-soo 1	Extracted	3 ch.	<i>Eriophorum vaginatum</i> , <i>Calluna vulgaris</i> , <i>Vaccinium uliginosum</i> , <i>Polytrichum strictum</i> , <i>Betula pubescens</i> , and <i>Pinus sylvestris</i>	57.914	26.697
Ess-soo 2	Extracted	3 ch.	<i>Oxycoccus palustris</i> , <i>Empetrum nigrum</i> , <i>Vaccinium uliginosum</i> , <i>Polytrichum strictum</i> , <i>Eriophorum vaginatum</i> , and <i>Calluna vulgaris</i>	57.913	26.687
Kildemaa					
Kildemaa 1	Extracted	3 ch.	<i>Eriophorum vaginatum</i> , <i>Calluna vulgaris</i> , <i>Rhynchospora alba</i> , <i>Betula pubescens</i> , and <i>Pinus sylvestris</i>	58.427	24.786
Kildemaa 2	Drained	3 ch.	<i>Calluna vulgaris</i> , <i>Ledum palustre</i> , <i>Polytrichum strictum</i> , <i>Andromeda polifolia</i> , and <i>Pinus sylvestris</i>	58.424	24.784
Kõima					
Kõima 1	Drained	3 ch.	Various <i>Sphagnum</i> species, <i>Calluna vulgaris</i> , <i>Ledum palustre</i> , <i>Rubus chamaemorus</i> , <i>Andromeda polifolia</i> , and <i>Pinus sylvestris</i>	58.617	24.233
Kõima 2	Natural	3 ch. at lawn	Various <i>Sphagnum</i> species, <i>Calluna vulgaris</i> , <i>Andromeda polifolia</i> , and <i>Pinus sylvestris</i>	58.614	24.239
Laiuse					
Laiuse 0	Extracted	4 ch.	<i>Polytrichum strictum</i> , <i>Eriophorum vaginatum</i> , <i>Calluna vulgaris</i> , <i>Betula pubescens</i> , and <i>Pinus sylvestris</i>	58.790	26.528
Laiuse 1	Extracted	3 ch.	<i>Polytrichum strictum</i> , <i>Eriophorum vaginatum</i> , <i>Calluna vulgaris</i> , and <i>Pinus sylvestris</i>	58.790	26.528
Laiuse water	Extracted	1 floating ch.		58.789	26.529
Linnussaare					
Linnussaare	Natural	3 ch. at hollows, 3 ch. at hummocks, 1 floating ch. in pool	Various <i>Sphagnum</i> species, <i>Ledum palustre</i> , <i>Vaccinium uliginosum</i> , <i>Calluna vulgaris</i> , and <i>Pinus sylvestris</i>	58.878	26.219
Maima					
Maima 1	Extracted	3 ch.	<i>Eriophorum vaginatum</i> , <i>Calluna vulgaris</i> , <i>Oxycoccus palustris</i> , <i>Vaccinium uliginosum</i> , <i>Betula pubescens</i> , and <i>Pinus sylvestris</i>	58.599	24.379
Maima 2	Extracted	3 ch.	<i>Eriophorum vaginatum</i> , <i>Rhynchospora alba</i> , <i>Calluna vulgaris</i> , and <i>Pinus sylvestris</i>	58.596	24.370
Männikjärve					
Männikjärve 1	Natural	2 ch. at hollows, 2 ch. at hummocks	Various <i>Sphagnum</i> species, <i>Calluna vulgaris</i> , <i>Chamaedaphne calyculata</i> , <i>Rhynchospora alba</i> , <i>Ledum palustre</i> , <i>Oxycoccus microcarpus</i> , and <i>Pinus sylvestris</i>	58.874	26.254
Männikjärve 2	Natural	2 ch. at hollows, 2 ch. at hummocks	Various <i>Sphagnum</i> species, <i>Calluna vulgaris</i> , <i>Oxycoccus microcarpus</i> , <i>Carex</i> , and <i>Pinus sylvestris</i>	58.876	26.249
Männikjärve 3	Natural	2 floating ch. in pool, 2 ch. at hummocks	Various <i>Sphagnum</i> species, <i>Calluna vulgaris</i> , <i>Oxycoccus microcarpus</i> , and <i>Pinus sylvestris</i>	58.876	26.247

peat extraction area is sparse and is dominated by *Eriophorum vaginatum*, *Calluna vulgaris*, *Empetrum nigrum*, *Vaccinium uliginosum*, *Polytrichum strictum*, *Betula pubescens*, and *Pinus sylvestris*.

The Kildemaa study site in the northern part of Kõrsa bog comprises an abandoned milled peat production site (remaining peat layer depth 0.8–2 m). A densely drained part of the bog was prepared for peat extraction but abandoned before extraction began (peat deposit up to 3 m). The extracted site is sparsely vegetated with



*E. vaginatum*, *C. vulgaris*, *Rhynchospora alba*, *B. pubescens*, and *P. sylvestris*, while the drained part is densely covered with dwarf pines (*P. sylvestris*), *C. vulgaris*, *Ledum palustre*, lichens, and mosses.

Kõima and Maima peatlands belong to the Lavassaare bog complex, where the peat deposit depth reaches 7.5 m. The Kõima study site covers a former peat extraction site and an adjacent nearly pristine reference site in the northwest part of Kõima bog. Peat was extracted by cutting the peat into blocks with a machine or by hand. The extraction site was abandoned in the 1980s and left for natural recovery. Ditches and depressions are mainly recovered with *Sphagnum* species and drained unexcavated parts are covered with *C. vulgaris*, *L. palustre*, *Rubus chamaemorus*, *Andromeda polifolia*, and *P. sylvestris*. In Maima, milled peat extraction took place until the 1990s, when it was abandoned. Currently, the site is only sparsely vegetated with *E. vaginatum*, *C. vulgaris*, *Oxycoccus palustris*, *V. uliginosum*, *B. pubescens*, and *P. sylvestris*.

Laiuse bog is of limnogenic origin and is situated between drumlins. Mining activity ceased there in 1996, and the peatland was left for natural regeneration. The northern part is partly covered with *P. strictum*, *E. vaginatum*, *C. vulgaris*, *B. pubescens*, and *P. sylvestris*, while the southern part has been flooded due to beaver activity since 2013.

Linnussaare and Männikjärve bogs belong to the Endla Nature Reserve and are included in the Ramsar List of Wetlands of International Importance (no. 907). These peatlands are of limnogenic origin; their peat layer varies from 4 to 7 m and consists of residuals of *Sphagnum*, Bryales, *Carex*, and *Pinus* (Sillasoo et al., 2007). Vegetation includes dwarf pines (*P. sylvestris*), grasses and dwarf shrubs (*C. vulgaris*, *E. vaginatum*, *Chamaedaphne calyculata*, *A. polifolia*, *R. alba*, *L. palustre*, *Oxycoccus microcarpus*, and *O. palustris*), and a wide variety of *Sphagnum* mosses (*Sphagnum fuscum*, *Sphagnum balticum*, *Sphagnum magellanicum*, and *Sphagnum rubellum*) (Burdun, Bechtold, Sagris, Komisarenko, et al., 2020).

## 2.2. Field Measurements of CO<sub>2</sub>, CH<sub>4</sub>, WTD, and Soil Temperature

We measured  $R_{\text{eco}}$  (CO<sub>2</sub>) with CH<sub>4</sub> fluxes with the closed-chamber method (Hutchinson & Livingston, 1993) during the snow-free period (March–November) in 2017–2020. Each chamber was measured multiple times over the growing season, although this varied between sites (see Figure 2 for further details). Chambers (40-cm height, 50-cm diameter, and 65-L volume) were made of white polyvinyl chloride (PVC) to minimize their heating. The chambers were sealed with water-filled PVC collars (20 cm depth) on the peat surface. Each sampling site had replicates (Table 1) and was instrumented with piezometers (perforated pipes with 5-cm diameter and up to 1.5-m length). We sampled gas using pre-evacuated (0.3 mbar) glass vials (50-mL volume) every 20 min during a 1-hr session. Later, the gas concentration in vials was measured using a Shimadzu GC-2014 gas chromatography system equipped with an electron capture detector and a flame ionization detector. WTD was measured in piezometers on the same days that gas samples were collected. Negative numbers for WTD data indicate a water table position below the peat surface, while positive numbers indicate flooding above the peat surface. In addition to WTD, we measured soil temperature at depths –10 cm ( $T_{10}$ ), –20 cm ( $T_{20}$ ), –30 cm ( $T_{30}$ ), and –40 cm ( $T_{40}$ ) and at the surface ( $T_0$ ).

## 2.3. Flux Calculation

Fluxes of CO<sub>2</sub> and CH<sub>4</sub> were calculated from the linear change in gas concentration in a chamber at 20-min intervals. We adjusted gas concentration by the surface area enclosed by collar and chamber volume. Afterward, we filtered out samples with a determination coefficient ( $R^2$ ) of the linear fit <0.95 ( $p$ -value < 0.01) except for the samples with fluxes changes below the gas-chromatographer accuracy (20 ppm for CO<sub>2</sub> and 20 ppb for CH<sub>4</sub>). Additionally, we filtered out CH<sub>4</sub> values higher than 30,000  $\mu\text{g C m}^{-2} \text{ h}^{-1}$  interpreted as ebullition fluxes. For the final analyses, we calculated the average CO<sub>2</sub> and CH<sub>4</sub> fluxes across replicates in each sampling position (Table 1). The flux data were grouped by peatlands' conditions and microtopographic characteristics, creating five groups: flooded sites (data from floating chambers in Männikjärve 3, Linnussaare, and Laiuse water), hollows (Männikjärve 1, Männikjärve 2, and Linnussaare), hummocks (Männikjärve 1 to Männikjärve 3, Linnussaare, and Kõima 2), drained sites (Kõima 1 and Kildemaa 2), and extracted sites (Ess-soo 0 to Ess-soo 2, Kildemaa 1, Laiuse 0, Laiuse 1, Maima 1, and Maima 2). Figure 2 shows the time series of CO<sub>2</sub> and CH<sub>4</sub> fluxes in 2017–2020 for those five groups.

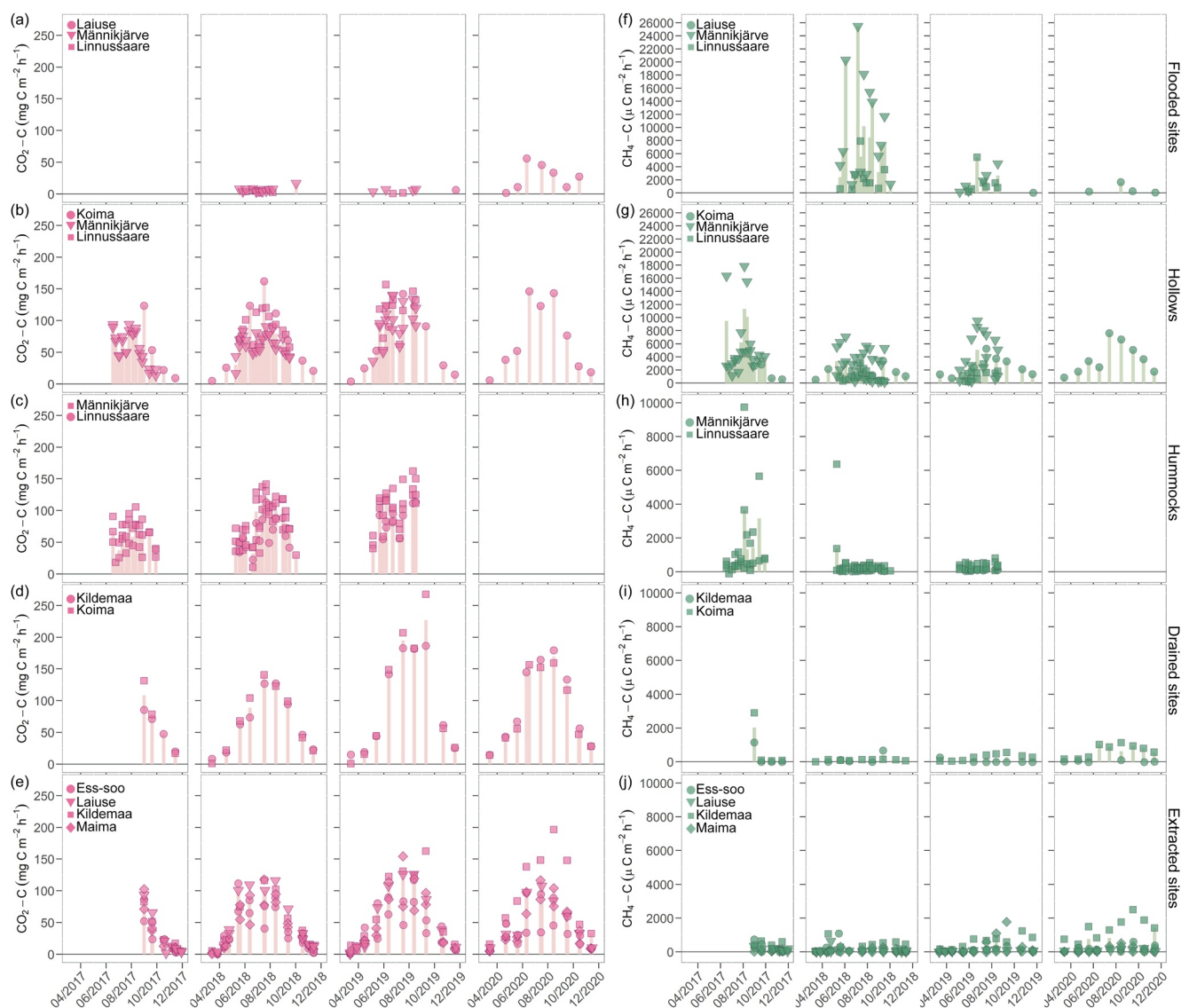


**Figure 2.** Time series of  $\text{CO}_2$  and  $\text{CH}_4$  fluxes: one time measured values (marks) and averaged for each day (bars) for flooded sites (a and f), hollows (b and g), hummocks (c and h), drained (d and i), and extracted sites (e and j).

## 2.4. Landsat and MODIS LST

We calculated LST from Landsat 7 and Landsat 8 data in the Google Earth Engine (GEE) online platform using open-source code by Ermida et al. (2020). This LST retrieval algorithm utilizes Landsat thermal infrared and optical data (to derive the normalized difference vegetation index, NDVI), total column water vapor values from NCEP/NCAR reanalysis data, and the ASTER GEDv3 data set to estimate surface emissivity. All these data sets are freely available in GEE (Gorelick et al., 2017).

The field sampling was carried out on the days when Landsat 7 or Landsat 8 passed over the study area. Because of cloudy weather conditions, we had to mask out many LST pixels around the sampling sites. Thus, we decided to calculate the median Landsat LST value over each peatland for each time scene (Figure 3). This decision not only increased data availability for analyses, but it also introduced uncertainty since Landsat LST values can vary up to  $6^\circ\text{C}$  within one peatland (Figure S1 in Supporting Information S1).

MODIS aboard Terra provides MOD11A1 daily LST at a 1-km spatial resolution (Wan et al., 2015). We masked pixels covered with clouds and shadows using the quality control band, which is included in the

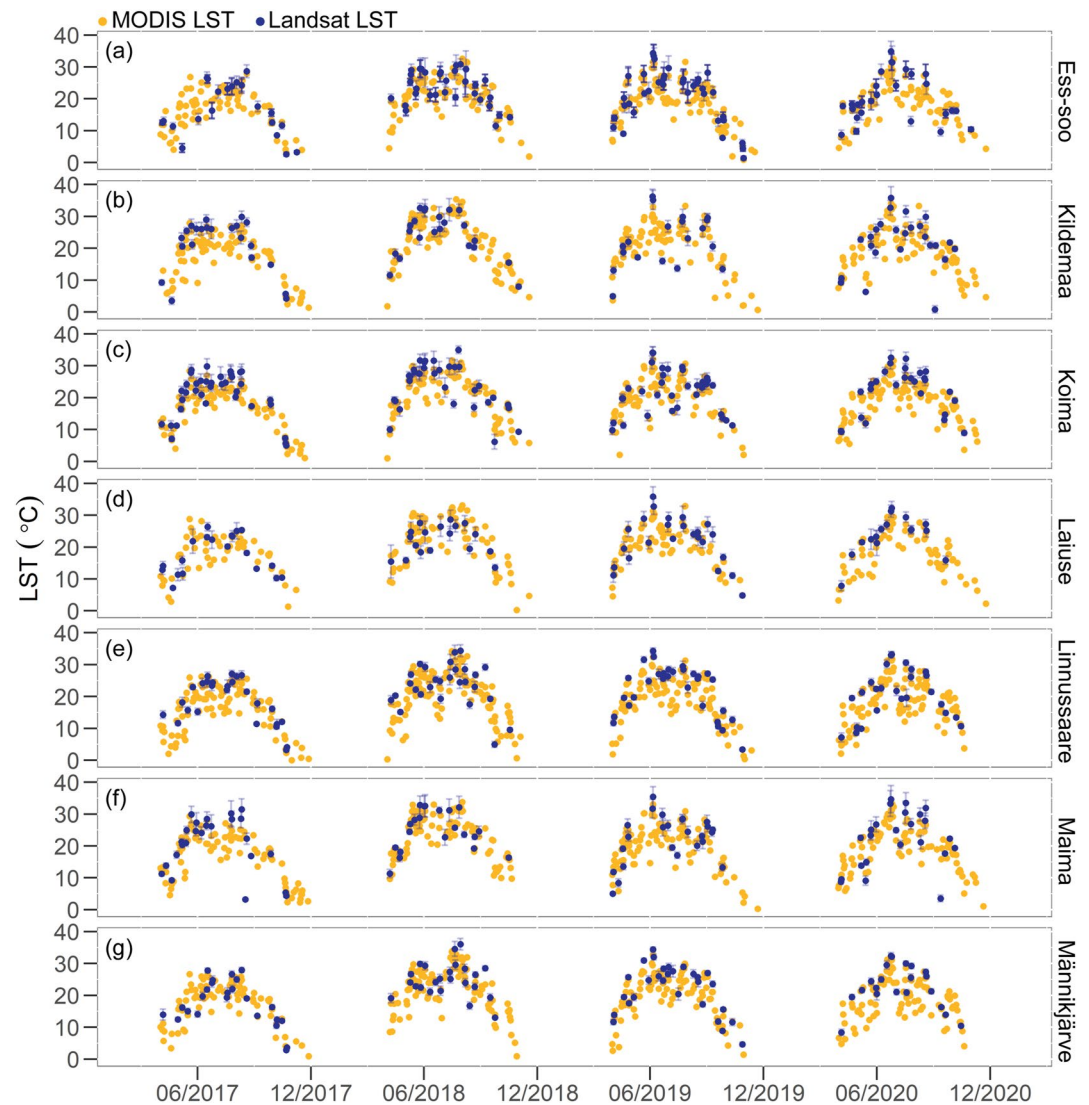


**Figure 3.** Time series of MODIS land surface temperature (LST) median (yellow circles), Landsat LST median values (blue circles), and Landsat LST standard deviation within peatland area (blue error bars) in Ess-soo (a), Kildemaa (b), Kõima (c), Laiuse (d), Linnussaare (e), Maima (f) and Männikjärve (g) peatlands.

MOD11A1 data set in GEE. As with Landsat LST data, we calculated the MODIS LST value as a median across all pixels that cover peatland for each time scene. MODIS LST values accorded well with Landsat LST values (Figure S2 in Supporting Information S1). Nevertheless, the slope of relationships between MODIS LST and Landsat LST varies from 0.778 to 0.887 for different peatlands. This means that under warmer conditions ( $>15^{\circ}\text{C}$ ), Landsat LST values are higher in comparison with MODIS LST values, and vice versa under cooler conditions: lower Landsat LST values in comparison with MODIS LST values.

In this study, we used remotely sensed MODIS data with a coarse spatial resolution and aggregated Landsat data. The use of these data leads to uncertainty regarding the spatial variation of LST data within the study peatlands. This uncertainty, in turn, raises the problem of representativeness of the LST values for the location where  $R_{\text{eco}}$  was measured. Mainly, this problem affects the sites with several types of land management (Kõima and Kildemaa) and sites with a high spatial variation of Landsat LST values (Ess-soo and Maima, Figure S1 in Supporting Information S1). Therefore, we acknowledge the bias arising from our data sources, while noting that this is offset by the long time-series availability and a high temporal resolution that are more critical within the scope of our study.

The final numbers of Landsat and MODIS images were, respectively, 167 and 420 for Ess-soo, 88 and 387 for Kildemaa, 131 and 387 for Kõima, 78 and 302 for Laiuse, 111 and 441 for Linnussaare, 95 and 379 for Maima, and 98 and 372 for Männikjärve (Figure 3).

## 2.5. $R_{eco}$ Modeling

We modeled  $R_{eco}$  following the approach developed by Lloyd and Taylor (1994) and modified by Tuittila et al. (2004). We utilized a model adjusted by Gaussian curve functions of a second term that account for additional WTD and phenological phase effects (Equation 1) as in previous reports (Järveoja et al., 2016; Riutta et al., 2007):

$$R_{eco} = R_{ref} e^{E_0 \left( \frac{1}{T_{ref} - T_{min}} - \frac{1}{T - T_{min}} \right)} \times e^{-0.5 \times \left( \frac{Pp - Pp_{opt}}{Pp_{tol}} \right)^2} \times e^{-0.5 \times \left( \frac{WTD - WTD_{opt}}{WTD_{tol}} \right)^2}, \quad (1)$$

where  $R_{ref}$  ( $\text{mg CO}_2 \text{ m}^{-2} \text{ h}^{-1}$ ) is the respiration rate at  $10^\circ\text{C}$ ,  $E_0$  (K) denotes temperature sensitivity,  $T_{ref}$  ( $^\circ\text{C}$ ) is a reference temperature set at  $10^\circ\text{C}$ ,  $T_{min}$  ( $^\circ\text{C}$ ) is temperature minimum at which respiration reaches zero set at  $-46.021^\circ\text{C}$ ,  $T$  is field-measured surface temperature,  $Pp$  (day) denotes the days in a phenological phase that starts in spring when the daily average air temperature is above  $5^\circ\text{C}$  (Jaagus & Ahas, 2000),  $Pp_{opt}$  (day) denotes the optimal day for maximum  $R_{eco}$  from the beginning of vegetation period,  $Pp_{tol}$  (day) is a vegetation period tolerance for maximum  $R_{eco}$ , and  $WTD_{opt}$  (cm) is an optimal soil water level for respiration and  $WTD_{tol}$  (cm) denotes the soil water-level tolerance (deviation from the optimum at which  $R_{eco}$  is 61% of its maximum).

Parameters utilized in Equation 1 were fitted with a Microsoft Excel Solver tool for calculation of the ecosystem respiration  $\text{CO}_2$ -response curve (Lobo et al., 2013). First, we derived the parameters utilizing surface temperature ( $T_0$ ) as  $T$  in Equation 1 for each sampling site separately and summarized them by groups (intact, drained, and extracted sites) as in a previous study (Turetsky et al., 2014). In doing so, we aimed to explore the intergroup variability of the fitted parameters. Afterward, we derived one set of fitted parameters using  $T_0$  for each of the three groups. In this way, we attempted to test the applicability of our model to estimate the  $R_{eco}$  for the specific peatland group, regardless of the spatial variability within each group (Olofsson et al., 2008; Wu et al., 2014; Xiao et al., 2010). After we estimated  $R_{eco}$  for specific peatland groups using  $T_0$  data, we modeled  $R_{eco}$  with MODIS LST data utilizing the same  $T_0$ -based fitted parameters. In this way, we assessed the interchangeability of in situ temperature and LST for  $R_{eco}$  modeling.

## 2.6. Statistical Analysis

Statistical analysis was performed in R software (R Core Team, 2020). We averaged the collar flux data for replicates at each site (Table 1) for further statistical analysis to avoid pseudoreplication. Furthermore, we applied principal component analysis (PCA) to derive information about the relationships among all variables measured in situ and cluster data, depending on the relevance of different variables for four studied groups, namely hummocks, hollows, and drained and extracted sites. Before PCA, the variables were standardized to zero mean. We did not include flooded sites in PCA since we did not measure the temporal variation of WTD or water column depth in ponds. Temporal changes in the water column depth affect  $\text{CH}_4$  and  $\text{CO}_2$  fluxes from ponds (Duchemin et al., 1995; McEnroe et al., 2009); therefore, PCA without this parameter would not be representative.

To estimate the common linear associations in paired repeated measures data, we calculated repeated measures correlation,  $\text{rmR}$  (Bakdash & Marusich, 2017), between  $\text{CO}_2$  and  $\text{CH}_4$  fluxes and in situ measured parameters, and between in situ temperatures, MODIS LST, and Landsat LST. The results of  $\text{rmR}$  were used to draw conclusions about the variability between data from different sampling sites but included in one group. Similar to the correlation coefficient,  $\text{rmR}$  varies from  $-1$  to  $1$ . However,  $\text{rmR}$  does not violate the assumption of independence of observations. Therefore, this method can be used to reveal the associations shared among individual observations in the aggregated data set. We calculated  $\text{rmR}$  using the  $\text{rmcorr}$  package (Bakdash & Marusich, 2017) in R software (R Core Team, 2020). Before  $\text{rmR}$  calculation, distributions of  $\text{CO}_2$  and  $\text{CH}_4$  data were normalized with Tukey's Ladder of Powers and log transformations, respectively.



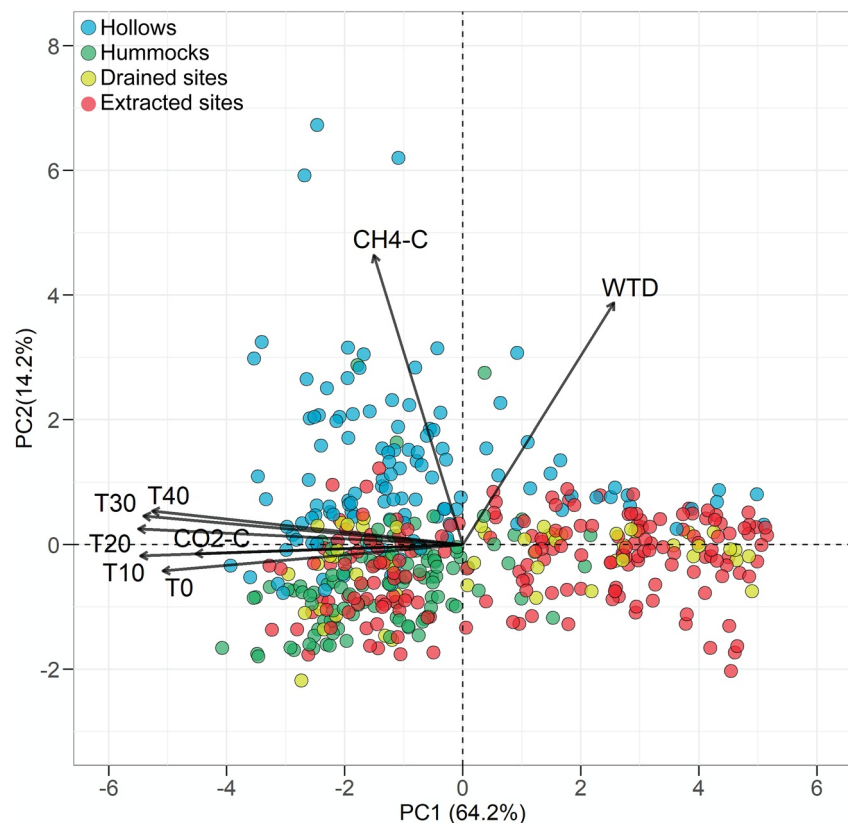


**Figure 4.** Principal component analysis for in situ measured data for hollows (blue), hummocks (green), drained (yellow), and extracted (red) sites. PC1 and PC2 correspond to the first two principal components (PCs).

The normality of transformed data was estimated visually with quantile-quantile plots. We calculated Pearson correlation ( $R$ ) for the data originating from one sampling site. Specifically, we provide  $R$  values between in situ temperatures and LST in the flooded site (Section 3.2) since only data from Männikjarve 3 sampling site were present. Both  $rmR$  and  $R$  were estimated with a  $p$ -value  $< 0.05$  indicating a statistical significance.

Owing to the higher temporal resolution of the MODIS LST product compared with Landsat LST, we estimated  $rmR$  between Landsat LST and  $T_0 - T_{40}$  only for intact sites. For the same reason, we did not perform  $R_{eco}$  modeling with Landsat LST data. Instead, MODIS LST was incorporated in the correlation analysis and  $R_{eco}$  modeling for all sites. The goodness of  $R_{eco}$  model performance was evaluated with  $R$ -squared ( $R^2$ ) and root-mean-square error (RMSE) statistics.

### 3. Results

#### 3.1. Environmental Controls on CO<sub>2</sub> and CH<sub>4</sub>

In Figure 4, the PCA of in situ data shows the separation between different peatland groups. The in situ data projected onto the first two principal components (PCs), which explain 78.4% of the variance in data. PC1 is correlated with temperatures and CO<sub>2</sub> fluxes, whereas PC2 is correlated with CH<sub>4</sub> fluxes and WTD. The distributions of intact (hummocks and hollows) and disturbed (drained and extracted) sites are well separated by high CH<sub>4</sub> fluxes and WTD. At the same time, the distributions of all four groups show a minor separation along PC1.

To compare the relations between CO<sub>2</sub> and CH<sub>4</sub> fluxes and in situ measured parameters, we performed repeated measures correlation analysis. Figure 5 shows the correlation matrices for the peatland groups. The flooded sites stand out from others because their CO<sub>2</sub> fluxes do not have any statistically significant relations with in situ parameters. However, CH<sub>4</sub> fluxes are positively associated with water temperature. In

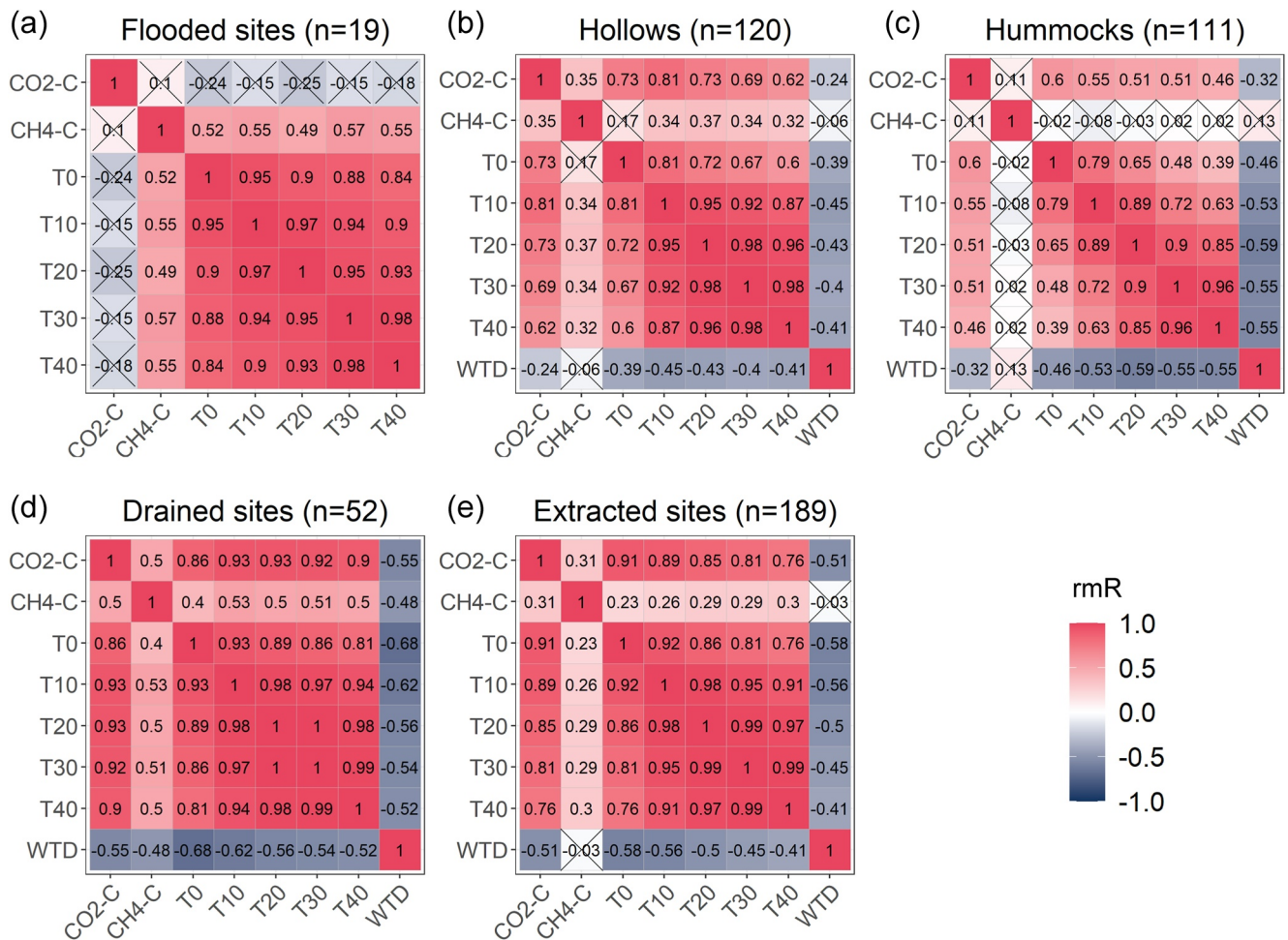


**Figure 5.** Repeated measures correlation (rmR) between CO<sub>2</sub> and CH<sub>4</sub> fluxes (normalized values), water table depth (WTD), and surface (T<sub>0</sub>) and soil (T<sub>10</sub>–T<sub>40</sub>) temperatures in flooded (a), hollows (b), hummocks (c), drained (d) and extracted (e) sites. Intense red and blue colors indicate strong positive and negative rmR values, respectively. Crossed-out cells correspond to rmR values with a p-value > 0.05.

other groups, CO<sub>2</sub> fluxes have weak to strong rmR with temperatures and WTD. In hollows and hummocks, CO<sub>2</sub> fluxes have higher rmR values with surface and soil temperatures than with WTD. Both hollows and hummocks show higher rmR with CO<sub>2</sub> fluxes for upper soil layers. It is further noteworthy that rmR values between CO<sub>2</sub> fluxes and T<sub>0</sub>–T<sub>40</sub> in drained and extracted sites are higher than those in intact sites. The highest rmR values for CO<sub>2</sub> fluxes are observed with T<sub>10</sub>–T<sub>30</sub> in drained sites.

Furthermore, Figure 6 shows the relations between T<sub>0</sub> and CO<sub>2</sub> and CH<sub>4</sub> fluxes for five groups. As previously shown in Figure 5, CO<sub>2</sub> fluxes are positively associated with temperature increases. Therefore, the maximum values of median CO<sub>2</sub> fluxes are observed in the summer months. In contrast, the lowest median values of CO<sub>2</sub> fluxes occur at the beginning of spring (March and April) and the end of autumn (October and November). Also, the weak negative association between CO<sub>2</sub> fluxes and WTD is noticeable in Figures 6b–6e. The positive association between CH<sub>4</sub> fluxes and T<sub>0</sub> can be seen for hollows and flooded, drained, and extracted sites (Figures 6f, 6g, 6i, and 6j). Similar to CO<sub>2</sub>, the highest median CH<sub>4</sub> fluxes occur in summer.

### 3.2. LST Versus In Situ Temperatures

The profiles of temperature at different depths together with remotely sensed Landsat and MODIS LST values are shown in Figure 7. We found that median peat temperatures decreased with depth; the highest temperature differential occurred between T<sub>0</sub> and T<sub>10</sub>. Drained and extracted sites have high variability in peat temperature with bimodal distribution (Figures 7d and 7e). In contrast, hummocks, hollows, and flooded

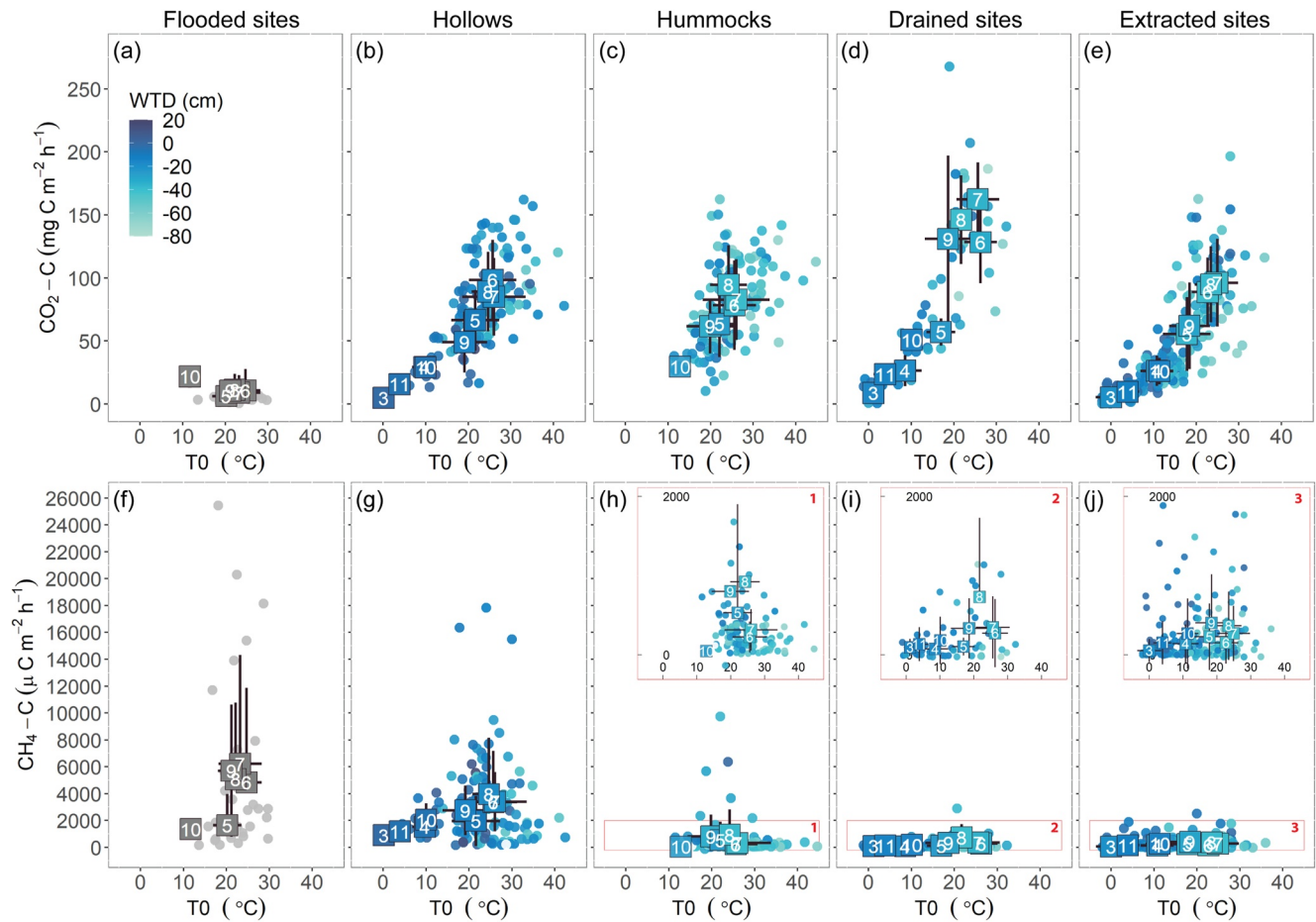


**Figure 6.** Scatterplots of surface temperature ( $T_0$ ),  $\text{CO}_2$ , and  $\text{CH}_4$  fluxes (circles) in flooded (a and f), hollows (b and g), hummocks (c and h), drained (d and i) and extracted (e and j) sites. Monthly fluxes and  $T_0$  averages (square shapes with month numbers) are also given with monthly standard deviations (error bars). Colors indicate the water table depth (WTD) except for flooded sites, where no WTD data are available. Inset graphs in panels (h–j) present zoomed-in areas in red rectangles. Negative numbers for WTD data indicate a water table position below the peat surface, while positive numbers indicate flooding above the peat surface.

sites have lower temperature variability and are close to the normal temperature distribution at almost all depths (Figures 7a–7c). Uneven measurement campaigns over time caused the difference in temperature distributions between drained and intact sites. As it is shown in Figure 2, the field data were collected once per month from March to November in one intact site (Kõima 2), all drained and extracted sites. However, the major amount of data from intact sites was collected in Linnussaare and Männikjärve peatlands once per several weeks from May to September. Therefore, we observe fewer low temperature values for early spring and late autumn in intact sites.

In Figure 7, the LST Landsat values are, on average, higher than MODIS LST values in intact peatlands. Moreover, MODIS LST had consistently higher rmR with in situ temperatures than Landsat LST (Figures 7a–7c). We expected the different performance of MODIS LST and Landsat LST since the slope of their relationships varies from 1.16 to 3.43 (Figure S2 in Supporting Information S1). However, despite the lower spatial resolution, MODIS LST demonstrated superiority over Landsat LST. The mean rmR values between in situ temperatures were 0.38 for Landsat LST and 0.47 for MODIS LST in hummocks and hollows. We further estimated rmR between LST and in situ measured temperatures. For all sites except flooded, both MODIS (Figures 7b–7e) and Landsat LST (Figures 7b and 7c) had the highest rmR with  $T_0$ . It is noteworthy that rmR between LST and in situ temperatures was higher for disturbed sites than for intact ones.

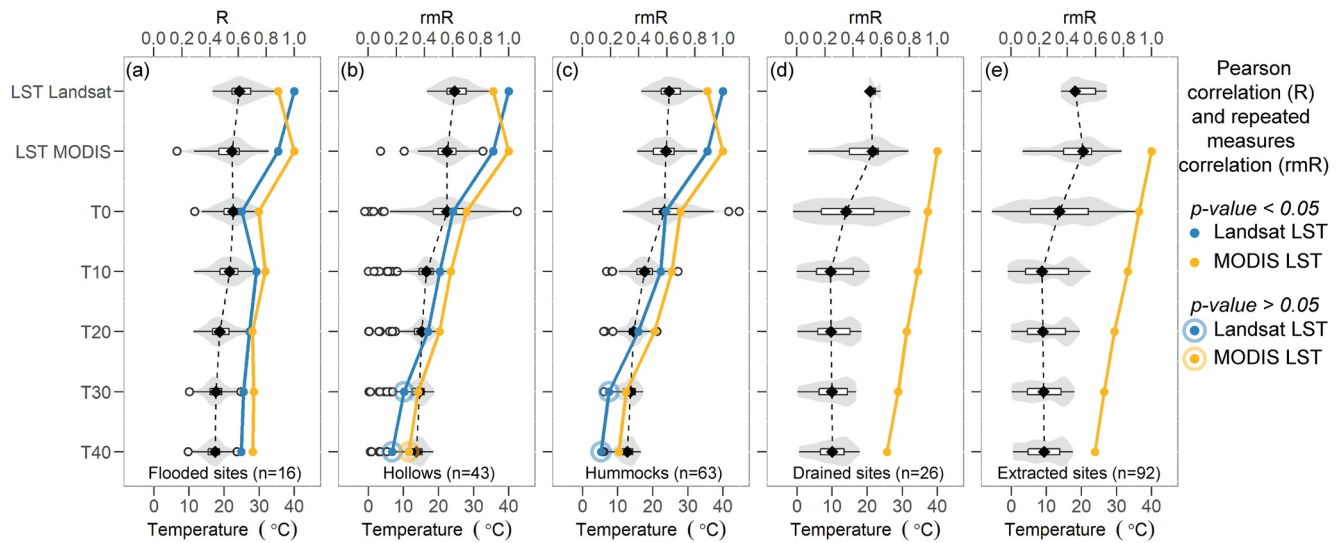


**Figure 7.** Profiles of temperature variation (boxplot) and distribution (shaded area) sensed by Landsat and MODIS, measured at the surface level ( $T_0$ ) and 10–40 cm depths in the peat ( $T_{10}$ – $T_{40}$ ) for five groups. The median values (black diamonds) for the mentioned temperatures are connected with a dashed line. Blue and orange dots represent Pearson correlation ( $R$ ) and repeated measures correlation ( $rmR$ ) between Landsat land surface temperature (LST) and MODIS LST, respectively, and in situ measured temperatures.

### 3.3. Modeling $R_{eco}$ With In Situ Measured $T_0$ and Remotely Sensed MODIS LST

To estimate the potential of LST to be used instead of in situ measured temperatures in  $R_{eco}$  modeling, we compared the performance of  $R_{eco}$  models driven by  $T_0$  and by MODIS LST data (Figure S3 in Supporting Information S1). At first, we fitted the parameters from Equation 1 utilizing  $T_0$  for each sampling site separately and summarized them according to three groups: intact, drained, and extracted sites (Table 2). By doing this, we explored the intergroup variability of the fitted parameters as well as groups' specificities.

Table 2 highlights that  $R_{eco}$  in intact sites is characterized by the highest temperature sensitivity and the lowest flux rate at 10°C. Additionally, we observe the widest vegetation period tolerance for maximum  $R_{eco}$  (mean 91.70 days) and the shallowest optimal WTD for intact sites.  $R_{eco}$  in disturbed sites has much lower temperature sensitivity and deeper optimal WTD with wider WTD tolerance. It should be noted that the drained sites have the highest respiration rate at 10°C, which agrees with the data shown in Figure 6d.

After we estimated the site-specific parameters, we derived one set of fitted parameters using  $T_0$  for each of the three groups (Table 3). It is noticeable that the group-specific parameters differ from the mean values of the parameters in Table 2. First, for the intact sites,  $E_0$  value was higher in a group-specific model (Table 3) than the mean one in the site-specific models. Additionally, in the site-specific models,  $E_0$  was lower for

**Table 2**

Mean and Standard Errors of Estimated Parameters for Ecosystem Respiration ( $R_{eco}$ ) Models Fitted for Each Sampling Site and Grouped by Peatland Conditions: Intact, Drained, and Extracted

Model parameter	Intact (hummock, hollow)	Drained	Extracted
$E_0$ (K)	201.78 ± 23.61	109.05 ± 22.65	132.00 ± 24.38
$R_{ref}$ (mg CO <sub>2</sub> m <sup>-2</sup> h <sup>-1</sup> )	56.18 ± 6.95	121.35 ± 13.85	69.10 ± 10.73
$Pp_{opt}$ (day)	104.80 ± 7.11	119.25 ± 3.25	100.00 ± 3.85
$Pp_{tol}$ (day)	91.70 ± 13.11	63.45 ± 2.25	71.70 ± 3.60
$WTD_{opt}$ (cm)	−18.95 ± 5.18	−30.10 ± 9.30	−34.00 ± 5.82
$WTD_{tol}$ (cm)	30.16 ± 4.35	32.60 ± 9.00	38.70 ± 6.50

Note. Negative values of  $WTD_{opt}$  indicate the water table position below the peat surface. WTD, water table depth.



**Table 3**  
*Parameters for Ecosystem Respiration ( $R_{eco}$ ) Model in Intact (Hummocks and Hollows Merged), Drained and Extracted Peatlands*

Model parameter	Intact (hummock, hollow)	Drained	Extracted
$E_0$	147.5	114.2	154.7
$R_{ref}$	50.9	113.8	64.4
$Pp_{opt}$	99.6	117.6	99
$Pp_{tol}$	105.5	62.5	71
$WTD_{opt}$	−28.7	−25.5	−20.7
$WTD_{tol}$	99	65.1	43.6

Note. WTD, water table depth.

hollows (average 169.48 K) than for hummocks (average 234.08 K) and varied from 120.3 K (hollows at Mannikjarve 1) to 300 K (hummocks at Mannikjarve 1).

Second, the group-specific  $WTD_{opt}$  values vary from the mean  $WTD_{opt}$  shown in Table 2. Nevertheless, they laid within the ranges of the minimum and maximum values of the site-specific  $WTD_{opt}$ . In intact sites, the site-specific  $WTD_{opt}$  values varied from −51.8 cm (Mannikjarve 2 hummocks) to −6 cm (Mannikjarve 1 hummocks). A similar range of site-specific  $WTD_{opt}$  variation was observed for the drained sites: from −50.9 cm (Ess-soo 1) to −11.2 cm (Maima 2).

Finally, in group-specific models for intact and drained sites,  $WTD_{tol}$  resulted in higher values than those in Table 2. This difference in  $WTD_{tol}$  originated from merging WTD data measured at different microtopographical units. The difference in surface altitude caused by hummock-

hollow microtopography resulted in a high spatial variation of WTD. As a result, the models for intact and drained groups resulted in a wide water-level tolerance. In comparison to intact sites, drained sites have a lower spatial variation of WTD caused by land subsidence.

To show the applicability of LST data for  $R_{eco}$  modeling in intact, drained, and extracted peatlands, we compared the  $R_{eco}$  modeled using (a)  $T_0$  data and (b) MODIS LST data. For modeling  $R_{eco}$  with  $T_0$  and MODIS LST, we utilized the parameters presented in Table 3. We found that  $R_{eco}$  values were modeled with higher accuracy for disturbed peatlands (Table 4). As shown in Figure 5,  $T_0$  has a strong relationship with  $CO_2$  fluxes in disturbed peatlands. Thus,  $R^2$  values for the model that utilized  $T_0$  were 0.75 for the whole data set and 0.70 for the days when MODIS LST data were available in drained sites. In extracted sites, those values were 0.70 and 0.66, correspondingly. Across the intact sites,  $R^2$  values were notably lower at 0.36 and 0.29. When we used MODIS LST instead of  $T_0$  in the model, we found a similar pattern:  $R^2$  was higher for the disturbed sites (0.67 in extracted sites and 0.66 in drained sites) than for the intact sites (0.27). It is worth noting that relatively high RMSE values were present in all models.

A comparison between measured and modeled  $CO_2$  fluxes reveals that we generally fail to catch the variability of  $CO_2$  in intact sites (Figure 8a). In particular, we observe that the modeling approach cannot be used with either  $T_0$  or MODIS LST to model  $CO_2$  fluxes higher than  $100 \text{ mg C m}^{-2} \text{ h}^{-1}$  in the intact sites. Meanwhile, modeled  $CO_2$  fluxes better agreed with measured ones in disturbed sites (Figures 8b and 8c). However, some obvious outliers are noticeable for the highest  $CO_2$  fluxes for which  $CO_2$  fluxes were modeled with lower values. We found that those outliers were present in the model output produced with  $T_0$  as well as with MODIS LST.

**Table 4**  
*Performance of Ecosystem Respiration ( $R_{eco}$ ) Models Driven by Surface Temperature ( $T_0$ ) and MODIS Land Surface Temperature (LST) in Intact (Hummocks and Hollows Merged), Drained, and Extracted Peatlands*

Model input	Model statistics	Intact (hummocks, hollows)	Drained	Extracted
$T_0^a$	$R^2$	0.36	0.75	0.70
	RMSE ( $\text{mg CO}_2 \text{ m}^{-2} \text{ h}^{-1}$ )	27.38	30.77	21.92
$T_0^b$	$R^2$	0.29	0.70	0.66
	RMSE ( $\text{mg CO}_2 \text{ m}^{-2} \text{ h}^{-1}$ )	29.23	37.26	24.06
MODIS LST	$R^2$	0.27	0.66	0.67
	RMSE ( $\text{mg CO}_2 \text{ m}^{-2} \text{ h}^{-1}$ )	29.59	39.27	23.71

Note. RMSE, root-mean-square error.

<sup>a</sup>For the whole data set. <sup>b</sup>For the days when MODIS LST data were available.

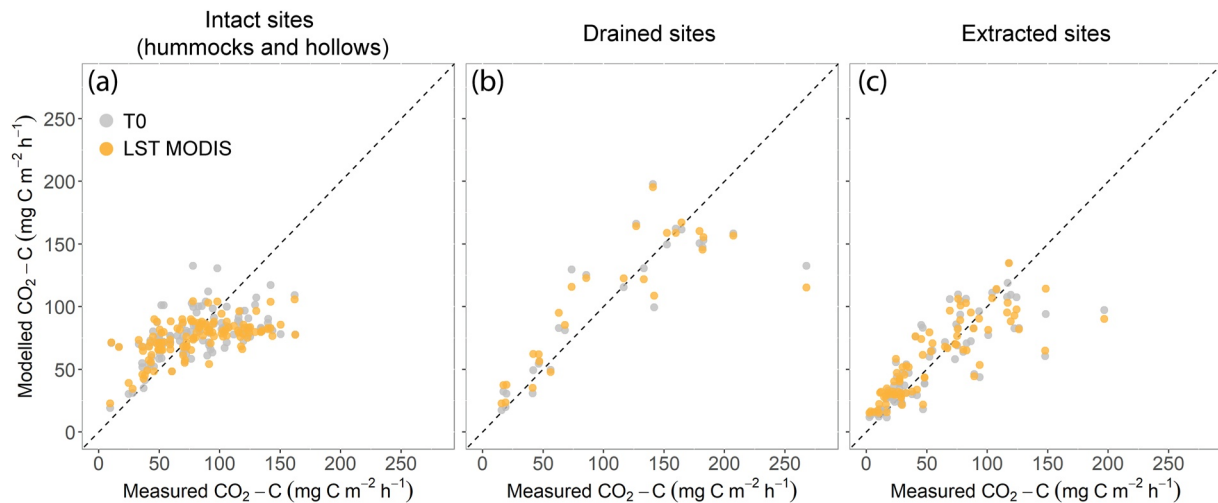


**Figure 8.**  $\text{CO}_2$  fluxes measured in situ and modeled with surface temperature— $T_0$  (gray circle)—and remotely sensed MODIS land surface temperature (LST) (orange circle) for intact (hummocks and hollows together), drained, and extracted sites. The dashed line shows a 1:1 relationship.

#### 4. Discussion

Prior studies have noted the importance of LST for  $R_{\text{eco}}$  estimations in different ecosystems. So far, none of the studies have addressed the potential of LST as a proxy for in situ measured temperatures for modeling  $R_{\text{eco}}$  in disturbed peatlands. Here, we enriched the current knowledge and provided evidence for the future application of LST for that purpose. Even though we utilized daytime MODIS LST data of a 1-km spatial resolution, we still managed to detect the temporal dynamics in temperatures measured in situ at a plot scale (Figure 7). This is particularly important for disturbed sites, where  $R_{\text{eco}}$  was mainly driven by thermal conditions (Figure 5).

Using the model parameterized for  $T_0$ , we utilized MODIS LST instead of  $T_0$  and obtained  $R^2$  equal to 0.27 for modeled  $R_{\text{eco}}$  in intact sites and 0.66 and 0.67 in drained and extracted sites, respectively. For comparison, in a previous study by Junttila et al. (2021) that jointly used remotely sensed LST and EVI data, the average  $R^2$  was 0.56 among five peatlands. The lowest  $R^2$  was obtained for the bog site (0.23), while  $R^2$  was dramatically higher for fen sites and varied from 0.51 to 0.85. We did not have a fen site in our data set; however, the modeling results for bogs are in line with those published by Junttila et al. (2021). Notably, the use of additional remotely sensed data (e.g., vegetation indices) could improve the  $R_{\text{eco}}$  model performance for intact peatlands. For instance, Schubert et al. (2010) obtained high  $R^2$  for both Swedish bog ( $R^2 = 0.89$ ) and fen ( $R^2 = 0.83$ ) by using LST, NDVI, and EVI data from MODIS. Ai et al. (2018) modeled  $R_{\text{eco}}$  utilizing LST and EVI for a big data set with nine wetland biomes and obtained  $R^2 = 0.59$ .

Generally, we observed a weak rmR between MODIS LST and Landsat LST and in situ temperatures and between in situ temperatures and  $\text{CO}_2$  and  $\text{CH}_4$  fluxes in intact sites. As previously shown for bogs (Burdun et al., 2019), LST has a weak to moderate association with soil temperatures, and the strength of this association decreases with soil depth. LST dynamics are highly dictated by incident solar radiation, while deeper soil temperatures slowly react with fewer fluctuations (R. Huang et al., 2020). Additionally, we assume that weak rmR between LST and  $T_{10}-T_{40}$  could be partially caused by a higher heat capacity of saturated peat in natural sites with shallow WTD (Zhao & Si, 2019). In previous work, Burdun et al. (2019) demonstrated that MODIS LST had higher rmR with  $T_{10}-T_{40}$  during summers with abnormally high temperatures and correspondingly deeper WTD.

Interestingly, the MODIS LST had consistently higher rmR with in situ temperatures than Landsat LST. The superiority of MODIS LST might arise from a more accurate emissivity estimation in the MODIS product (Ermiida et al., 2020). Nevertheless, both MODIS LST and Landsat LST reveal weaker rmR with  $T_0$  in intact sites. We believe this was primarily caused by vegetation cover properties. The studied intact bogs are covered with dense vegetation, primarily Sphagnum mosses, which demonstrate high water loss by

evapotranspiration, which approaches the potential rate of open water evaporation (Kim & Verma, 1996). Through evapotranspiration, mosses cool the surface and perform as a thermal insulation layer (Blok et al., 2011). For these reasons, the disturbed sites with deeper WTD, covered with sporadic vegetation and open peat surface, had higher rmR between LST and  $T_0-T_{40}$ .

In situ temperatures had strong rmR with  $\text{CO}_2$  fluxes in disturbed sites but not in intact ones (Figure 5). This weaker rmR in intact sites could be explained by the significant effect of soil moisture on  $\text{CO}_2$  production (Waddington et al., 2001). Both peat temperature and moisture regulate the biological processes underlying  $\text{CO}_2$  production (Alm et al., 2007). However, soil moisture has a much larger effect on  $\text{CO}_2$  production in natural peatlands than in disturbed ones (Waddington et al., 2001). Waddington et al. (2001) observed a peak in  $\text{CO}_2$  production rate at approximately 92% saturation in the upper peat layer. This means that the disturbed peatlands with deeper WTD may rarely reach this value of saturation. Most of the time, their surface moisture remains far from  $\text{CO}_2$  production optimum. The highest rmR between  $\text{CO}_2$  and peat temperatures in the intact sites was obtained for  $T_0-T_{10}$ . In our study,  $T_0-T_{10}$  correspond to the uppermost peat soil layer, which has previously been shown to have the largest  $\text{CO}_2$  production rates (Lafleur et al., 2005).

In the current study, we performed site- and group-specific modeling of  $R_{\text{eco}}$ . Based on the modeling results, we found a high inner-group variation of the site-specific parameters. This high variation resulted in discrepancies between the mean site-specific parameters shown in Table 2 and group-specific parameters in Table 3. Overall, the modeled group-specific parameters laid within the ranges of the minimum and maximum values of these site-specific parameters. The intact sites had the highest mean  $E_0$  in Table 2; however, in the group-specific model, their  $E_0$  value decreased and became lower than the  $E_0$  modeled for the extracted sites. We hypothesize that differences in  $E_0$  and  $\text{WTD}_{\text{tol}}$  values presented in Tables 2 and 3 can be explained by the variation in surface altitude and surface heterogeneity between the sites within one group.

In contrast, we did not observe the high discrepancies for  $R_{\text{ref}}$ ,  $\text{Pp}_{\text{opt}}$ , and  $\text{Pp}_{\text{tol}}$  parameters in site- and group-specific models.  $R_{\text{ref}}$  parameter was found to be the highest for the drained sites in Tables 2 and 3. This high respiration rate can be explained by strong relationships between temperature, heterotrophic, and autotrophic respiration (Pries et al., 2015). The drained sites have a higher heterotrophic respiration than the intact ones due to the deeper WTD (Figure 6) (Jaatinen et al., 2008). Additionally, the drained sites have a higher autotrophic respiration than the extracted ones due to the denser vegetation cover (Järveoja et al., 2016). The combination of both these types of respiration could have resulted in the observed high  $R_{\text{ref}}$  value for the drained sites. Drained sites had later  $\text{Pp}_{\text{opt}}$  and the narrower  $\text{Pp}_{\text{tol}}$  than the intact sites, which can be explained by the difference in vegetation cover. Drained sites were covered with vascular plants that have late start of the photosynthesis period (Korrensalo et al., 2017). In contrast, intact sites were dominantly covered with Sphagnum mosses that start their photosynthesis activity early in the spring (Korrensalo et al., 2017).

In this work,  $R_{\text{eco}}$  models were driven by in situ measurements, among which were WTD time series. However, only a small number of peatlands have in situ historical observations, which limit the future applicability of the provided model. Therefore, remotely sensed proxies of WTD must be used, such as radar data (Asmuß et al., 2019; Tampuu et al., 2020) and Optical Trapezoid Model (Burdun, Bechtold, Sagris, Lohila, et al., 2020). Furthermore, given the well-established respiration dependency on LST in disturbed sites, future work could focus on the benefits of combining various remotely sensed data. For example, LAI, NDVI, and EVI were shown to increase the  $R_{\text{eco}}$  model accuracy over various biomes, including peatlands (Ai et al., 2018; Y. Gao et al., 2015; Junttila et al., 2021). Additionally, vegetation indices have the potential to be utilized as proxies of  $\text{Pp}_{\text{opt}}$  and  $\text{Pp}_{\text{tol}}$  parameters, since indices can indicate the ecosystem productivity (Dronova et al., 2021). Moreover, the parameterization of models separately for each peatland could increase the model performance (Junttila et al., 2021).

In accordance with previous works (Evans et al., 2021; Feng et al., 2020), in all the sites, rmR between  $\text{CH}_4$  fluxes and in situ measured parameters was weak and moderate (from  $-0.5$  to  $0.5$ ) and periodically not statistically significant ( $p\text{-value} > 0.05$ ). The highest correlation (rmR =  $0.53$ ) was observed between  $\text{CH}_4$  fluxes and  $T_{10}$  in drained sites. Additionally, we observed a positive association ( $p\text{-value} > 0.05$ ) between  $\text{CH}_4$  fluxes and water temperature in flooded sites. In Figure 2, it is noticeable that  $\text{CH}_4$  fluxes follow seasonal dynamics in flooded sites (panel f). Summer 2018 was warmer than summer 2019, so  $\text{CH}_4$  fluxes increased

dramatically during 2018 and were the greatest in midsummer. Similar results were discussed in a study by McEnroe et al. (2009), in which a weak positive ( $p$ -value < 0.001)  $R$  was found between air temperature and  $\text{CH}_4$  fluxes.

Our findings may be somewhat limited by the small number of sites and methodological constraints. First, we tested LST applicability in only seven sites where  $R_{\text{eco}}$  data were measured with the closed-chamber technique. A well-known possibility is that chamber measurements of  $R_{\text{eco}}$  might not accurately represent the fluxes at the landscape scale (Schrier-Uijl et al., 2010). Second, we applied MODIS LST data of a 1-km spatial resolution. The MODIS pixels' footprint covered neighboring territories around the peatlands, which could cause bias in the association between in situ measured  $R_{\text{eco}}$  and LST. We did not utilize Landsat LST for  $R_{\text{eco}}$  modeling because of the very limited number of cloud-free images for the disturbed sites. This lack of data occurred even though we calculated one median Landsat LST value over one site for each time scene to increase the amount of Landsat LST data. Unfortunately, high latitudes—where 80% of peatland C stock is located (Tanneberger et al., 2017)—are frequently covered by clouds. In this regard, modeling  $R_{\text{eco}}$  with high-resolution Landsat data is challenging in northern peatlands. A good alternative to the original Landsat LST data could be modeled Landsat LST data derived with temporal adaptive reflectance fusion model, such as STARFM (F. Gao et al., 2006). The fusion algorithms for Landsat and MODIS imagery have already shown promising results (Moreno-Martinez et al., 2020). Additionally, machine learning techniques could be used to fill the gaps in Landsat LST images (Buo et al., 2021).

Altogether, our results highlight that remotely sensed LST is a powerful tool for modeling  $R_{\text{eco}}$ , particularly in disturbed peatlands. LST has the potential to be used in drained and extracted sites with deep WTD and those covered with sparse sedges or bare peat surface. However, more studies are needed to identify how our findings are generalizable across disturbed peatlands in the Northern Hemisphere.

## 5. Conclusions

The purpose of this study was to estimate the strength of the relationships between  $R_{\text{eco}}$  and LST in disturbed (drained and extracted) and intact peatlands. In particular, we aimed to examine the applicability of MODIS LST for  $R_{\text{eco}}$  modeling and compare the performance of the MODIS LST-driven model with the model driven by the in situ measured surface temperature. This study indicates that LST has a great potential to be utilized in  $R_{\text{eco}}$  models as a proxy of thermal conditions in northern peatlands. The highest rmR (mean 0.78) was observed between MODIS LST and the in situ measured  $T_0$ – $T_{40}$  for drained and extracted sites. However, in intact sites, the relationships between LST and  $T_0$ – $T_{40}$  were dramatically weaker: mean rmR over hummocks and hollows was 0.38 for Landsat and 0.49 for MODIS. The  $R_{\text{eco}}$  model driven by MODIS LST yielded similar accuracy to the model driven by in situ  $T_0$ :  $R^2$  was 0.29, 0.70, and 0.66, respectively, for intact (hummocks and hollows), drained, and extracted sites with the  $T_0$ -driven model and 0.27, 0.66, and 0.67, respectively, with the MODIS LST-driven model.

The present study represents one of the first attempts to thoroughly examine the potential of remotely sensed LST for monitoring C fluxes of drained and extracted peatlands. Although our study was limited to only seven peatlands with an intermittent  $R_{\text{eco}}$  time series based on the manual closed-chamber technique, we showed that LST data could be used as a tool to monitor  $\text{CO}_2$  fluxes with relatively high accuracy. Future research should be carried out to identify how generalizable our findings are across disturbed peatlands in the Northern Hemisphere.

## Data Availability Statement

Field measured data, reported in this study, are available at Zenodo: <https://doi.org/10.5281/zenodo.5118730>.

## References

- Acosta, M., Juszczak, R., Chojnicki, B., Pavelka, M., Havránková, K., Lesny, J., et al. (2017).  $\text{CO}_2$  fluxes from different vegetation communities on a peatland ecosystem. *Wetlands*, 37(3), 423–435. <https://doi.org/10.1007/s13157-017-0878-4>
- Ai, J., Jia, G., Epstein, H. E., Wang, H., Zhang, A., & Hu, Y. (2018). MODIS-based estimates of global terrestrial ecosystem respiration. *Journal of Geophysical Research: Biogeosciences*, 123(2), 326–352. <https://doi.org/10.1002/2017JG004107>

## Acknowledgments

The authors are grateful to Dr Alar Teemusk for gas sample analyses at the laboratory of the Department of Geography, Institute of Ecology and Earth Sciences, University of Tartu, Estonia. The authors acknowledge the kind support of three anonymous reviewers and the editor; their input in increasing the quality and clarity of the manuscript is invaluable. This work was financially supported by the Estonian Research Council (research grants PRG-352 and MOBERC20), the European Commission through the European Regional Development Fund (the Center of Excellence EcolChange), and the European Commission and ETAG for funding ERA-NET Cofund project WaterJPI-JC-2018\_13: ReformWater and the Estonian State Forest Management Centre (project LLTOM17250 “Water level restoration in cut-away peatlands: development of integrated monitoring methods and monitoring,” 2017–2023).



- Alm, J., Shurpali, N. J., Minkinen, K., Aro, L., Hytönen, J., Laurila, T., et al. (2007). Emission factors and their uncertainty for the exchange of CO<sub>2</sub>, CH<sub>4</sub> and N<sub>2</sub>O in Finnish managed peatlands. *Boreal Environment Research*, 12, 191–209.
- Asmuß, T., Bechtold, M., & Tiemeyer, B. (2019). On the potential of sentinel-1 for high resolution monitoring of water table dynamics in grasslands on organic soils. *Remote Sensing*, 11(14), 1659. <https://doi.org/10.3390/rs11141659>
- Bakdash, J. Z., & Marusich, L. R. (2017). Repeated measures correlation. *Frontiers in Psychology*, 8. <https://doi.org/10.3389/fpsyg.2017.00456>
- Blok, D., Heijmans, M., Schaepman-Strub, G., van Ruijven, J., Parmentier, F. J. W., Maximov, T. C., & Berendse, F. (2011). The cooling capacity of mosses: Controls on water and energy fluxes in a Siberian Tundra site. *Ecosystems*, 14(7), 1055–1065. <https://doi.org/10.1007/s10021-011-9463-5>
- Bubier, J. L., Bhatia, G., Moore, T. R., Roulet, N. T., & Lafleur, P. M. (2003). Spatial and temporal variability in growing-season net ecosystem carbon dioxide exchange at a large peatland in Ontario, Canada. <https://doi.org/10.1007/s10021-003-0125-0>
- Buo, I., Sagris, V., & Jaagus, J. (2021). Gap-filling satellite land surface temperature over heatwave periods with machine learning (pp. 1–5). IEEE Geoscience and Remote Sensing Letters. <https://doi.org/10.1109/LGRS.2021.3068069>
- Burdun, I., Bechtold, M., Sagris, V., Komisarenko, V., De Lannoy, G., & Mander, Ü. (2020). A comparison of three trapezoid models using optical and thermal satellite imagery for water table depth monitoring in Estonian bogs. *Remote Sensing*, 12(12), 1–24. <https://doi.org/10.3390/rs12121980>
- Burdun, I., Bechtold, M., Sagris, V., Lohila, A., Humphreys, E., Desai, A., et al. (2020). Localizing pixels with SWIR-based moisture index representative of overall peatland water table dynamics. *Remote Sensing*.
- Burdun, I., Kull, A., Maddison, M., Veber, G., Karasov, O., Sagris, V., & Mander, Ü. (2021). CO<sub>2</sub> and CH<sub>4</sub> gas fluxes in disturbed and intact northern peatlands (Data set). <https://doi.org/10.5281/zenodo.5118730>
- Burdun, I., Sagris, V., & Mander, Ü. (2019). Relationships between field-measured hydrometeorological variables and satellite-based land surface temperature in a hemiboreal raised bog. *International Journal of Applied Earth Observation and Geoinformation*, 74, 295–301. <https://doi.org/10.1016/j.jag.2018.09.019>
- Change, I. P. on C. (2013). Anthropogenic and natural radiative forcing. In *Climate change 2013 the physical science basis: Working group I contribution to the fifth assessment report of the intergovernmental panel on climate change* (pp. 659–740). Cambridge University Press. <https://doi.org/10.1017/CBO9781107415324.018>
- Clymo, R. S., Turunen, J., & Tolonen, K. (1998). Carbon accumulation in peatland. *Oikos*, 81(2), 368. <https://doi.org/10.2307/3547057>
- Crabbe, R. A., Janouš, D., Dařenová, E., & Pavelka, M. (2019). Exploring the potential of LANDSAT-8 for estimation of forest soil CO<sub>2</sub> efflux. *International Journal of Applied Earth Observation and Geoinformation*, 77, 42–52. <https://doi.org/10.1016/j.jag.2018.12.007>
- Davidson, S. J., Strack, M., Bourbonniere, R. A., & Waddington, J. M. (2019). Controls on soil carbon dioxide and methane fluxes from a peat swamp vary by hydrogeomorphic setting. *Ecohydrology*, 12(8), e2162. <https://doi.org/10.1002/eco.2162>
- Dronova, I., Taddeo, S., Hemes, K. S., Knox, S. H., Valach, A., Oikawa, P. Y., et al. (2021). Remotely sensed phenological heterogeneity of restored wetlands: Linking vegetation structure and function. *Agricultural and Forest Meteorology*, 296, 108215. <https://doi.org/10.1016/j.AGRFORMET.2020.108215>
- Duchemin, E., Lucotte, M., Canuel, R., & Chamberland, A. (1995). Production of the greenhouse gases CH<sub>4</sub> and CO<sub>2</sub> by hydroelectric reservoirs of the boreal region. *Global Biogeochemical Cycles*, 9(4), 529–540. <https://doi.org/10.1029/95GB02202>
- Ermida, S. L., Soares, P., Mantas, V., Götsche, F.-M., & Trigo, I. F. (2020). Google Earth Engine open-source code for land surface temperature estimation from the Landsat series. *Remote Sensing*, 12(9), 1471. <https://doi.org/10.3390/rs12091471>
- Estonian Land Board. (2020). Orthophotos. Retrieved from [https://geoportaal.maaamet.ee/index.php?page\\_id=309&lang\\_id=2](https://geoportaal.maaamet.ee/index.php?page_id=309&lang_id=2)
- Estonian Weather Service. (2021). Estonian weather service. Retrieved from <https://www.ilmateenistus.ee/?lang=en>
- Evans, C. D., Peacock, M., Baird, A. J., Artz, R. R. E., Burden, A., Callaghan, N., et al. (2021). Overriding water table control on managed peatland greenhouse gas emissions. *Nature*, 593, 548–552. <https://doi.org/10.1038/s41586-021-03523-1>
- Feng, X., Deventer, M. J., Lonchar, R., Ng, G. H. C., Sebestyen, S. D., Roman, D. T., et al. (2020). Climate sensitivity of peatland methane emissions mediated by seasonal hydrologic dynamics. *Geophysical Research Letters*, 47(17), e2020GL088875. <https://doi.org/10.1029/2020GL088875>
- Gao, F., Masek, J., Schwaller, M., & Hall, F. (2006). On the blending of the landsat and MODIS surface reflectance: Predicting daily landsat surface reflectance. *IEEE Transactions on Geoscience and Remote Sensing*, 44(8), 2207–2218. <https://doi.org/10.1109/TGRS.2006.872081>
- Gao, Y., Yu, G., Li, S., Yan, H., Zhu, X., Wang, Q., et al. (2015). A remote sensing model to estimate ecosystem respiration in Northern China and the Tibetan Plateau. *Ecological Modelling*, 304, 34–43. <https://doi.org/10.1016/j.ecolmodel.2015.03.001>
- Gorelick, N., Hancher, M., Dixon, M., Ilyushchenko, S., Thau, D., & Moore, R. (2017). Google Earth Engine: Planetary-scale geospatial analysis for everyone. *Remote Sensing of Environment*, 202, 18–27. <https://doi.org/10.1016/j.rse.2017.06.031>
- Günther, A., Barthelmes, A., Huth, V., Joosten, H., Jurasinski, G., Koebisch, F., & Couwenberg, J. (2020). Prompt rewetting of drained peatlands reduces climate warming despite methane emissions. *Nature Communications*, 11(1), 1–5. <https://doi.org/10.1038/s41467-020-15499-z>
- Hanson, P. J., Griffiths, N. A., Iversen, C. M., Norby, R. J., Sebestyen, S. D., Phillips, J. R., et al. (2020). Rapid net carbon loss from a whole-ecosystem warmed peatland. *AGU Advances*, 1(3), e2020AV000163. <https://doi.org/10.1029/2020AV000163>
- Helbig, M., Humphreys, E. R., & Todd, A. (2019). Contrasting temperature sensitivity of CO<sub>2</sub> exchange in peatlands of the Hudson Bay Lowlands, Canada. *Journal of Geophysical Research: Biogeosciences*, 124(7), 2126–2143. <https://doi.org/10.1029/2019JG005090>
- Huang, N., Gu, L., Black, T. A., Wang, L., & Niu, Z. (2015). Remote sensing-based estimation of annual soil respiration at two contrasting forest sites. *Journal of Geophysical Research: Biogeosciences*, 120(11), 2306–2325. <https://doi.org/10.1002/2015JG003060>
- Huang, N., Gu, L., & Niu, Z. (2014). Estimating soil respiration using spatial data products: A case study in a deciduous broadleaf forest in the Midwest USA. *Journal of Geophysical Research: Atmospheres*, 119(11), 6393–6408. <https://doi.org/10.1002/2013JD020515>
- Huang, R., Huang, J. X., Zhang, C., Ma, H. Y., Zhuo, W., Chen, Y. Y., et al. (2020). Soil temperature estimation at different depths, using remotely-sensed data. *Journal of Integrative Agriculture*, 19(1), 277–290. [https://doi.org/10.1016/S2095-3119\(19\)62657-2](https://doi.org/10.1016/S2095-3119(19)62657-2)
- Huang, X., Silvennoinen, H., Klöve, B., Regina, K., Kandel, T. P., Playda, A., et al. (2021). Modelling CO<sub>2</sub> and CH<sub>4</sub> emissions from drained peatlands with grass cultivation by the BASGRA-BGC model. *Science of the Total Environment*, 765, 144385. <https://doi.org/10.1016/j.scitotenv.2020.144385>
- Hutchinson, G. L., & Livingston, G. P. (1993). Use of chamber systems to measure trace gas fluxes (pp. 63–78). John Wiley & Sons, Ltd. <https://doi.org/10.2134/soilscisocpub55.c4>
- Jaagus, J., & Ahas, R. (2000). Space-time variations of climatic seasons and their correlation with the phenological development of nature in Estonia. *Climate Research*, 15(3), 207–219. <https://doi.org/10.3354/cr015207>

- Jaatinen, K., Laiho, R., Vuorenmaa, A., Castillo, U. D., Minkinen, K., Pennanen, T., et al. (2008). Responses of aerobic microbial communities and soil respiration to water-level drawdown in a northern boreal fen. *Environmental Microbiology*, 10(2), 339–353. <https://doi.org/10.1111/J.1462-2920.2007.01455.X>
- Jägermeyr, J., Gerten, D., Lucht, W., Hostert, P., Migliavacca, M., & Nemani, R. (2014). A high-resolution approach to estimating ecosystem respiration at continental scales using operational satellite data. *Global Change Biology*, 20(4), 1191–1210. <https://doi.org/10.1111/gcb.12443>
- Järveoja, J., Nilsson, M. B., Crill, P. M., & Peichl, M. (2020). Bimodal diel pattern in peatland ecosystem respiration rebuts uniform temperature response. *Nature Communications*, 11(1), 1–9. <https://doi.org/10.1038/s41467-020-18027-1>
- Järveoja, J., Peichl, M., Maddison, M., Soosaar, K., Vellak, K., Karofeld, E., et al. (2016). Impact of water table level on annual carbon and greenhouse gas balances of a restored peat extraction area. *Biogeosciences*, 13(9), 2637–2651. <https://doi.org/10.5194/bg-13-2637-2016>
- Junttila, S., Kelly, J., Kljun, N., Aurela, M., Klemetsson, L., Lohila, A., et al. (2021). Upscaling northern peatland CO<sub>2</sub> fluxes using satellite remote sensing data. *Remote Sensing*, 13(4), 818. <https://doi.org/10.3390/rs13040818>
- Kim, J., & Verma, S. B. (1996). Surface exchange of water vapour between an open sphagnum fen and the atmosphere. *Boundary-Layer Meteorology*, 79(3), 243–264. <https://doi.org/10.1007/bf00119440>
- Kimball, J. S., Jones, L. A., Zhang, K., Heinsch, F. A., McDonald, K. C., & Oechel, W. C. (2009). A satellite approach to estimate land-atmosphere CO<sub>2</sub> exchange for boreal and Arctic biomes using MODIS and AMSR-E. *IEEE Transactions on Geoscience and Remote Sensing*, 47(2), 569–587. <https://doi.org/10.1109/TGRS.2008.2003248>
- Korrensalo, A., Alekseychik, P., Hájek, T., Rinne, J., Vesala, T., Mehtätalo, L., et al. (2017). Species-specific temporal variation in photosynthesis as a moderator of peatland carbon sequestration. *Biogeosciences*, 14(2), 257–269. <https://doi.org/10.5194/bg-14-257-2017>
- Kotta, J., Herkül, K., Jaagus, J., Kaasik, A., Raudsepp, U., Alari, V., et al. (2018). Linking atmospheric, terrestrial and aquatic environments: Regime shifts in the Estonian climate over the past 50 years. *PLoS One*, 13(12), e0209568. <https://doi.org/10.1371/journal.pone.0209568>
- Lafleur, P. M., Moore, T. R., Roulet, N. T., & Frolking, S. (2005). Ecosystem respiration in a cool temperate bog depends on peat temperature but not water table. *Ecosystems*, 8(6), 619–629. <https://doi.org/10.1007/s10021-003-0131-2>
- Lafleur, P. M., Roulet, N. T., & Admiral, S. W. (2001). Annual cycle of CO<sub>2</sub> exchange at a bog peatland. *Journal of Geophysical Research*, 106(D3), 3071–3081. <https://doi.org/10.1029/2000JD900588>
- Lees, K. J., Quaife, T., Artz, R. R. E., Khomik, M., & Clark, J. M. (2018). Potential for using remote sensing to estimate carbon fluxes across northern peatlands—A review. *Science of the Total Environment*, 615, 857–874. <https://doi.org/10.1016/j.scitotenv.2017.09.103>
- Leifeld, J., & Menichetti, L. (2018). The underappreciated potential of peatlands in global climate change mitigation strategies. *Nature Communications*, 9(1), 1–7. <https://doi.org/10.1038/s41467-018-03406-6>
- Leifeld, J., Wüst-Galley, C., & Page, S. (2019). Intact and managed peatland soils as a source and sink of GHGs from 1850 to 2100. *Nature Climate Change*, 9(12), 945–947. <https://doi.org/10.1038/s41558-019-0615-5>
- Lloyd, J., & Taylor, J. A. (1994). On the temperature dependence of soil respiration. *Functional Ecology*, 8(3), 315. <https://doi.org/10.2307/2389824>
- Lobo, F. de A., de Barros, M. P., Dalmagro, H. J., Dalmolin, Â. C., Pereira, W. E., de Souza, É. C., et al. (2013). Fitting net photosynthetic light-response curves with Microsoft Excel—A critical look at the models. *Photosynthetica*, 51(3), 445–456. <https://doi.org/10.1007/s11099-013-0045-y>
- Loisel, J., Gallego-Sala, A. V., Amesbury, M. J., Magnan, G., Anshari, G., Beilman, D. W., et al. (2021). Expert assessment of future vulnerability of the global peatland carbon sink. *Nature Climate Change*, 11(1), 70–77. <https://doi.org/10.1038/s41558-020-00944-0>
- Maljanen, M., Sigurdsson, B. D., Guömundsson, J., Öskarsson, H., Huttunen, J. T., & Martikainen, P. J. (2010). Greenhouse gas balances of managed peatlands in the Nordic countries present knowledge and gaps. *Biogeosciences*, 7(9), 2711–2738. <https://doi.org/10.5194/bg-7-2711-2010>
- McEnroe, N. A., Roulet, N. T., Moore, T. R., & Garneau, M. (2009). Do pool surface area and depth control CO<sub>2</sub> and CH<sub>4</sub> fluxes from an ombrotrophic raised bog, James Bay, Canada? *Journal of Geophysical Research*, 114(G1), G01001. <https://doi.org/10.1029/2007JG000639>
- Moreno-Martinez, A., Izquierdo-Verdiguier, E., Camps-Valls, G., Moneta, M., Munoz-Mari, J., Robinson, N., et al. (2020). Down-scaling MODIS vegetation products with Landsat GAP filled surface reflectance in Google Earth Engine (pp. 2320–2323). International Geoscience and Remote Sensing Symposium (IGARSS). <https://doi.org/10.1109/IGARSS39084.2020.9324007>
- Ojanen, P., Minkinen, K., & Penttilä, T. (2013). The current greenhouse gas impact of forestry-drained boreal peatlands. *Forest Ecology and Management*, 289, 201–208. <https://doi.org/10.1016/j.foreco.2012.10.008>
- Olofsson, P., Lagergren, F., Lindroth, A., Lindström, J., Klemetsson, L., Kutsch, W., & Eklundh, L. (2008). Towards operational remote sensing of forest carbon balance across Northern Europe. *Biogeosciences*, 5(3), 817–832. <https://doi.org/10.5194/bg-5-817-2008>
- Pan, Y., Birdsey, R. A., Fang, J., Houghton, R., Kauppi, P. E., Kurz, W. A., et al. (2011). A large and persistent carbon sink in the world's forests. *Science*, 333(6045), 988–993. <https://doi.org/10.1126/science.1201609>
- Park, H., Takeuchi, W., & Ichii, K. (2020). Satellite-based estimation of carbon dioxide budget in tropical peatland ecosystems. *Remote Sensing*, 12(2), 250. <https://doi.org/10.3390/rs12020250>
- Pries, C. E. H., van Logtestijn, R. S. P., Schuur, E. A. G., Natali, S. M., Cornelissen, J. H. C., Aerts, R., & Dorrepaal, E. (2015). Decadal warming causes a consistent and persistent shift from heterotrophic to autotrophic respiration in contrasting permafrost ecosystems. *Global Change Biology*, 21(12), 4508–4519. <https://doi.org/10.1111/GCB.13032>
- Rahman, A. F., Sims, D. A., Cordova, V. D., & El-Masri, B. Z. (2005). Potential of MODIS EVI and surface temperature for directly estimating per-pixel ecosystem C fluxes. *Geophysical Research Letters*, 32(19). <https://doi.org/10.1029/2005GL024127>
- R Core Team. (2020). *R: A language and environment for statistical computing*. Retrieved from <https://www.r-project.org/>
- Regan, S., Flynn, R., Gill, L., Naughton, O., & Johnston, P. (2019). Impacts of groundwater drainage on peatland subsidence and its ecological implications on an Atlantic raised bog. *Water Resources Research*, 55(7), 6153–6168. <https://doi.org/10.1029/2019WR024937>
- Rinne, J., Tuovinen, J. P., Klemetsson, L., Aurela, M., Holst, J., Lohila, A., et al. (2020). Effect of the 2018 European drought on methane and carbon dioxide exchange of northern mire ecosystems: 2018 drought on northern mires. *Philosophical Transactions of the Royal Society B: Biological Sciences*, 375(1810), 20190517. <https://doi.org/10.1098/rstb.2019.0517>
- Riutta, T., Laine, J., & Tuittila, E. S. (2007). Sensitivity of CO<sub>2</sub> exchange of fen ecosystem components to water level variation. *Ecosystems*, 10(5), 718–733. <https://doi.org/10.1007/s10021-007-9046-7>
- Salm, J.-O., Kimmel, K., Uri, V., & Mander, Ü. (2009). Global warming potential of drained and undrained Peatlands in Estonia: A synthesis. *Wetlands*, 29(4), 1081–1092. <https://doi.org/10.1672/08-206.1>
- Salm, J.-O., Maddison, M., Tammik, S., Soosaar, K., Truu, J., & Mander, Ü. (2012). Emissions of CO<sub>2</sub>, CH<sub>4</sub> and N<sub>2</sub>O from undisturbed, drained and mined peatlands in Estonia. *Hydrobiologia*, 692(1), 41–55. <https://doi.org/10.1007/s10750-011-0934-7>

- Scharlemann, J. P. W., Tanner, E. V. J., Hiederer, R., & Kapos, V. (2014). Global soil carbon: Understanding and managing the largest terrestrial carbon pool. *Carbon Management*, 5(1), 81–91. <https://doi.org/10.4155/cmt.13.77>
- Schrier-Uijl, A. P., Kroon, P. S., Hensen, A., Leffelaar, P. A., Berendse, F., & Veenendaal, E. M. (2010). Comparison of chamber and eddy covariance-based CO<sub>2</sub> and CH<sub>4</sub> emission estimates in a heterogeneous grass ecosystem on peat. *Agricultural and Forest Meteorology*, 150(6), 825–831. <https://doi.org/10.1016/j.agrformet.2009.11.007>
- Schubert, P., Eklundh, L., Lund, M., & Nilsson, M. (2010). Estimating northern peatland CO<sub>2</sub> exchange from MODIS time series data. *Remote Sensing of Environment*, 114(6), 1178–1189. <https://doi.org/10.1016/j.rse.2010.01.005>
- Sillasoo, U., Mauquoy, D., Blundell, A., Charman, D., Blaauw, M., Daniell, J. R. G., et al. (2007). Peat multi-proxy data from Männikjärve bog as indicators of late Holocene climate changes in Estonia. *Boreas*, 36(1), 20–37. <https://doi.org/10.1111/j.1502-3885.2007.tb01177.x>
- Swindles, G. T., Morris, P. J., Mullan, D. J., Payne, R. J., Roland, T. P., Amesbury, M. J., et al. (2019). Widespread drying of European peatlands in recent centuries. *Nature Geoscience*, 12(11), 922–928. <https://doi.org/10.1038/s41561-019-0462-z>
- Tampuu, T., Praks, J., Uiboupin, R., & Kull, A. (2020). Long term interferometric temporal coherence and DInSAR phase in northern peatlands. *Remote Sensing*, 12(10), 1566. <https://doi.org/10.3390/rs12101566>
- Tang, X., Liu, D., Song, K., Munger, J. W., Zhang, B., & Wang, Z. (2011). A new model of net ecosystem carbon exchange for the deciduous-dominated forest by integrating MODIS and flux data. *Ecological Engineering*, 37(10), 1567–1571. <https://doi.org/10.1016/j.ecoleng.2011.03.030>
- Tanneberger, F., Tegetmeyer, C., Busse, S., Barthelmes, A., Shumka, S., Mariné, A. M., et al. (2017). The peatland map of Europe. *Mires & Peat*, 19. <https://doi.org/10.19189/MaP.2016.OMB.264>
- Tuittila, E.-S., Vasander, H., & Laine, J. (2004). Sensitivity of C sequestration in reintroduced sphagnum to water-level variation in a cutaway peatland. *Restoration Ecology*, 12(4), 483–493. <https://doi.org/10.1111/j.1061-2971.2004.00280.x>
- Turetsky, M. R., Kotowska, A., Bubier, J., Dise, N. B., Crill, P., Hornibrook, E. R. C., et al. (2014). A synthesis of methane emissions from 71 northern, temperate, and subtropical wetlands. *Global Change Biology*, 20(7), 2183–2197. <https://doi.org/10.1111/gcb.12580>
- Veber, G., Kull, A., Villa, J. A., Maddison, M., Paal, J., Oja, T., et al. (2018). Greenhouse gas emissions in natural and managed peatlands of America: Case studies along a latitudinal gradient. *Ecological Engineering*, 114, 34–45. <https://doi.org/10.1016/j.ecoleng.2017.06.068>
- Waddington, J. M., Rotenberg, P. A., & Warren, F. J. (2001). Peat CO<sub>2</sub> production in a natural and cutover peatland: Implications for restoration. *Biogeochemistry*, 54(2), 115–130. <https://doi.org/10.1023/A:1010617207537>
- Waddington, J. M., & Roulet, N. T. (2000). Carbon balance of a boreal patterned peatland. *Global Change Biology*, 6(1), 87–97. <https://doi.org/10.1046/j.1365-2486.2000.00283.x>
- Wan, Z., Hook, S., & Hulley, G. (2015). MOD11A1 MODIS/Terra land surface temperature/emissivity daily L3 global 1km SIN grid V006. NASA EOSDIS Land Processes DAAC. <https://doi.org/10.5067/MODIS/MOD11A1.006>
- Wu, C., Gaumont-Guay, D., Andrew Black, T., Jassal, R. S., Xu, S., Chen, J. M., & Gonsamo, A. (2014). Soil respiration mapped by exclusive use of MODIS data for forest landscapes of Saskatchewan, Canada. *ISPRS Journal of Photogrammetry and Remote Sensing*, 94, 80–90. <https://doi.org/10.1016/j.isprsjprs.2014.04.018>
- Xiao, J., Zhuang, Q., Law, B. E., Chen, J., Baldocchi, D. D., Cook, D. R., et al. (2010). A continuous measure of gross primary production for the conterminous United States derived from MODIS and AmeriFlux data. *Remote Sensing of Environment*, 114(3), 576–591. <https://doi.org/10.1016/j.rse.2009.10.013>
- Xu, C., Qu, J. J., Hao, X., Zhu, Z., & Gutenberg, L. (2020). Monitoring soil carbon flux with in-situ measurements and satellite observations in a forested region. *Geoderma*, 378, 114617. <https://doi.org/10.1016/j.geoderma.2020.114617>
- Xu, J., Morris, P., Liu, J., & Holden, J. (2018). PEATMAP: Refining estimates of global peatland distribution based on a meta-analysis. *Catena*, 160, 134–140. <https://doi.org/10.1016/j.catena.2017.09.010>
- Yu, Z. (2011). Holocene carbon flux histories of the world's peatlands. *The Holocene*, 21(5), 761–774. <https://doi.org/10.1177/0959683610386982>
- Yu, Z., Loisel, J., Brosseau, D. P., Beilman, D. W., & Hunt, S. J. (2010). Global peatland dynamics since the Last Glacial Maximum. *Geophysical Research Letters*, 37(13). <https://doi.org/10.1029/2010GL043584>
- Zhao, Y., & Si, B. (2019). Thermal properties of sandy and peat soils under unfrozen and frozen conditions. *Soil and Tillage Research*, 189, 64–72. <https://doi.org/10.1016/j.still.2018.12.026>